KYAMBOGO UNIVERSITY

GRADUATE SCHOOL

DEPARTMENT OF MECHANICAL & PRODUCTION ENGINEERING

RESEARCH PROJECT THESIS

DETERMINATION OF COOLING EFFECTS ON TENSILE STRENGTH OF RE-BARS USING SPRAY QUENCHING.

BY

OMARA WALTER LOUIS

(16/U/13442/GMEM/PE)

AUGUST, 2019

RESEARCH THESIS

DETERMINATION OF COOLING EFFECTS ON TENSILE STRENGTH OF REBARS USING SPRAY QUENCHING.

OMARA WALTER LOUIS

(16/U/13442/GMEM/PE)

SUPERVISORS:
Dr. Titus BitekWatmon
Mr. Joseph Olwa

A Project Report Submitted to the Graduate School in Partial Fulfillment of the Requirements for the Award of Master of Science in Advanced Manufacturing Systems Engineering of Kyambogo University

AUGUST, 2019

ABSTRACT

In this study, the tensile strength in carbon steel was achieved under controlled heating and cooling processes. Forty-five samples of billets were used to produce 12 mm, 16 mm and 20 mm of hot-rolled rebar and each rebar was accorded different heat treatment process. The treatment process involved spray quenching by varying the coolant flow rate and coolant temperatureat 25^0C, 35^0C, and 45^0 C where the flow rate was controlled using pressure flow meter at 5Kgf/cm^2, 10 Kgf/cm^{2,} and 14 Kgf/cm^2. The samples for chemical analysis were prepared according to RRM-QA.WI-07and analyzed using the mass spectrometer.The tensile test specimens were prepared according to ASTM E8/E8M-13 and tests were conducted on the Universal Testing Machine. Microstructure analysis was carried out on the specimens obtained from samples using standard methods on a metallurgical microscope(Krussoptronic VOPC93) equipped with a camera of 3.0 megapixels. The analysis of chemical composition revealed that the samples are of low carbon steel with 0.233 wt.% C, 98.3 wt.% Fe, 0.746 wt.% Mn, 0.313 wt.% Si and other alloying elements. The results of the study showed that a pressure flow of 10 Kg f/cm^2, and coolant temperature of 35℃, is sufficient to cool a 12 mm, 16 mm and 20 mm rebar and obtain UTS values of 648 Mpa, 604 Mpa& 557 Mpa respectively which falls within 550-650 Mpa, as stipulated in the Ugandan Standard and East African Standard(US & EAS 412-2:2013). The results showed reduced strength for all rebar sizes at low-pressure flow of 5 Kgf/cm^{2}and high coolant temperature of 45^0C. The microstructure of the specimen showed that a matrix mix of pearlite and ferrite exists in the structure. The more the pearlite in the mixture, the more the hardness with increased strength and reduced percentage elongation, while the more the ferrite in the matrix mix, the less strength it exhibits and increased percentage elongation with less brittleness. The study also showed that for a 12 mm, 16 mm & 20 mm rebar, requires a range from 33.5^0C to 44.5^0C at 10 Kgf/cm^2 to 14 Kgf/cm^2, 35.5^0C to 44.5^0C at 6.8 Kgf/cm^2 to 13.2 Kgf/cm^2 and 26^0C to 43^0C at 6.3 Kgf/cm^2 to 13.3 Kgf/cm^2 respectively to produce UTS of 648-556 Mpa, 554-643 Mpa and 558-645 Mpa respectively. Implementation of these research results will help to reduce rejects of rebars and improve on financial loss of RRM.

Key words; heat treatment, spray quenching, mechanical properties, hot rolled steel bar

DECLARATION

I Omara Walter Louis declare that the work embodied in this dissertation is my own and has never been presented in any institution for an academic award. Where I have used the works of other persons, due acknowledgment and sources are provided.

Signature……. Date ……..

APPROVAL

This is to certify that the student has written this report, and it has been found to be the student's original work.

It is now ready for submission to the academic board of examiners of KYu with my due approval

Dr. Titus BitekWatmon

Signature…….

Date …….

Mr. Olwa Joseph

Signature…….

Date …….

DEDICATION

To my wife, Mr's Hudline Omara, children, Olwa Emmanuel, Okite Jerome, and Akullu Gloria.

ACKNOWLEDGMENT

I would like to acknowledge the power of the almighty God for the gift of life and protection from any form of the accident he has offered freely through the entire course of studies and data collection, glory is to God. I would also like to acknowledge the overwhelming academic support and effective supervision provided by my supervisors, Dr. Titus BitekWatmon and Mr. Joseph Olwa, Technicians and Engineers of Roofing Rolling Mill for their technical guidance during data collection. Furthermore, the Department of Mechanical and Production Engineering for allowing me to carryout research in this area, the management and staffs of Roofing Rolling Mill for allowing me to use their facilities feely and the University at large for accepting me to undertake this program and employing competent staff who guided me well and exposed me in this field of study. Not forgetting the family members and friends for their patience, financial support and time given to partake this course and has enabled the thesis to be accomplished in time.

I thank them all.

TABLE OF CONTENTS

LIST OF FIGURES

LIST OF TABLES

LIST OF APPENDICES

NOMENCLATURE

Kyu	Kyambogo University
RRM	Roofing Rolling Mills Ltd
UTM	Universal Testing Machine
HSLA	High Strength Low Alloy Steel
DPS	Dual Phase Steel
UTS	Ultimate Tensile Strength
YS	Yield Strength
AISI	American Iron and Steel Institute
SAE	Society of Automotive Engineers
ASTM	American Society for Testing and Materials
UNS	Uniform Numbering System,
TMT	Thermo Mechanical Treatment
TEM	Transmission Electron Microscope
FIE	Fuel Instrument Engineers

RRM-QA.WI-07 Roofing Rolling Mill Quality Assurance Working Instruction

CHAPTER ONE

INTRODUCTION

Determination of Cooling effects on Tensile Strength of Rebars using Spray Quenching

This chapter introduces the study by providing the background, statement of the problem, the purpose of the study, objectives, research questions, contribution of the study, Justification, conceptual framework, scope, the significance of the study limitation and mitigation.

1.0 Background

Roofings Rolling Mills (RRM) has been operating in Uganda since 1994 and was formerly known as Roofings Limited, located in Lubowa. It is the leading manufacturer of a wide range of steel and plastic construction materials applicable in the construction of bridges, railway lines, beams and columns for buildings, support structures, reinforced rods in concrete, etcused throughout the East and Central African region. According to the founder of Roofing Limited *(Sikander 2014)* the company started by importing already coated mild steel sheets from Russia, South Africa, and Europe which were then cut and sold without processing. The company by then had a capacity of 35,000 metric tons per annum.

However, in 2010 there was increasing demand for steel in the region and the company could not satisfy the market due to heavy cost involved in importing &transportation of raw materials and the limited space of the warehouses,it became difficult to expand the business until the company secured a new location at Kampala Industrial Business Park Namanve, where it started phase I and phase II dealing in wire galvanizing and hot rolling mill respectively. Phase 1 has a capacity of 12,000 metric tonnes per annum while phase II has a capacity to produce 72,000 metric tons of billets per annum.

Steel is basically alloys of iron and according to ASME (2002) steel can be defined as an alloy of iron, carbon (< 2% C) and other alloying elements like Fe, C, Mn, Si, P, S, Cr, Ni, Mo and other elements in various proportion, that is capable of being hot and /or cold deformed into various shapes. Steel consists of many alloying elements. The quality of steel depends largely on the cooling parameters like coolant temperature, quenching time, type of coolant, and diameter of the product, therefore alteration of these cooling parameters have varied significant impact on the quality of the product and can lead to huge amount of rejects and financial losses.

Song (2015),Tadayon&Varahram (2007),Valeria et al (2015) and others have presented papers on the effects of heat treatment on the mechanical properties of dual phase steels, ductile Iron and other types of steel using spray quenching heat treatment, their results showed improved mechanical and physical properties, however, the researchers did not answer the question of what effect will result if the product diameter, coolant temperature and coolant pressureare varied. All these independent parameters requireinvestigation for improved heat treatment process and quality of product in the market.This paper discusses the effect of spray quenching heat treatment on the mechanical characteristics and physical properties of hot rolled steel bars.

1.1Statement of the Problem

The Roofing Rolling Mill (RRM) produces an average reject of 200 pieces of rebar per 8 hour production run and yet it sells each rebar at Ugx. Shs. 35,000 on the market, thereby causing an annual financial loss of Ugx. Shs.7,560,000,000 due to imbalanced cooling during the production run, a maximum of 20 pieces of rejects per 8 hour production run is allowable by the company due to start-up loses which accounts for amiga annual financial loss of Ugx. Shs. 756,000,000 therefore there is need to determine the effects of cooling on strength of the rebar so as to establish a proper setting for cooling in order to drastically reduce the mega financial loss of the company.

1.2 Conceptual frame work

The rebar size, coolant temperature, coolant flow rate were manuplated to cause variation in Ulitmate Tensile strength, Yield strength, Percentage elongation, Microstructure of rebars. The strength of the out come was achieved through the plant efficiency and the efficiency of the testing equipments, while the variables which were kept constant through out the entire

experiments were coolant pressure, coolant temperature and time spent per rebar size in the quench box. The variables that influenced both the independent and dependent variables were temperature of the rebar at the furnance exit, chemical composition of the batch and the cooling rate as shown Figure:1-1

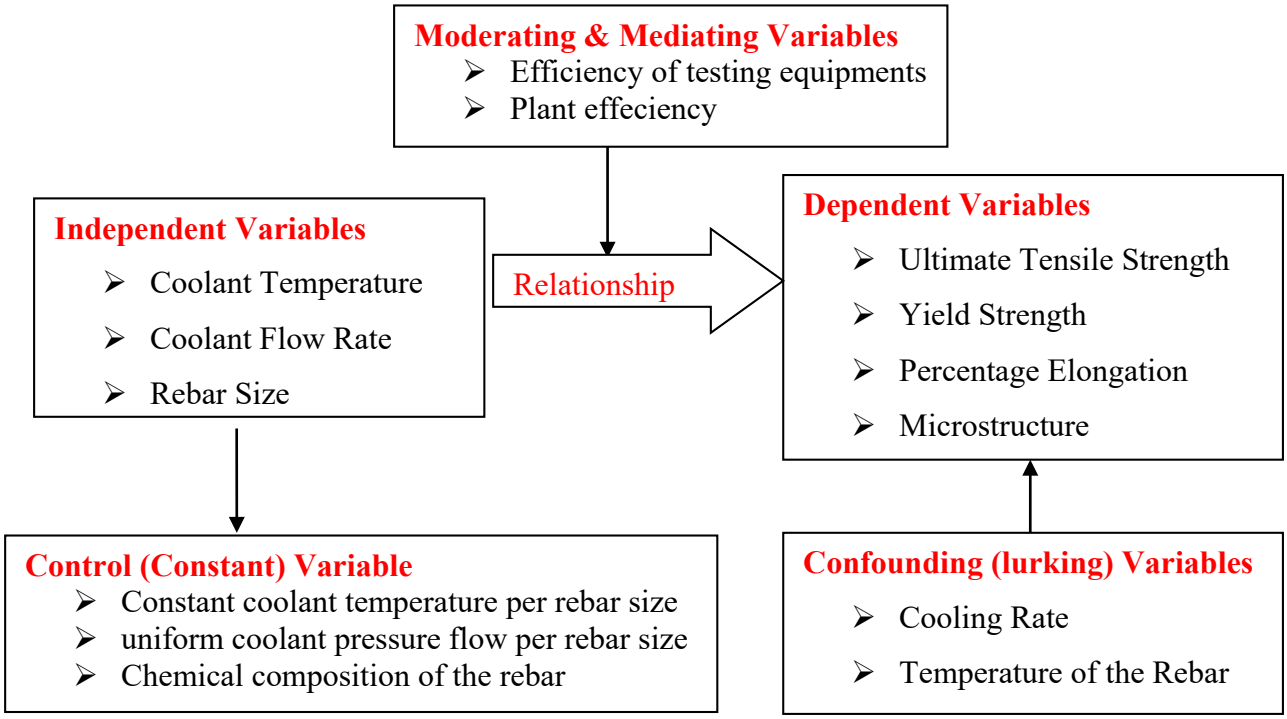

Figure1.1: Conceptual frame work

1.3Main Objective

The purpose of the research is to determine the effects of flow rate and coolant temperature on the tensile strength and establish a proper setting for cooling different sizes of the rebar.

1.4Specific Objectives

1) To determine the chemical composition of the billets.
2) To determine the effect of altering cooling parameters on tensile strength of the rebar.
3) To determine the effect of altering cooling parameters on microstructure of hot rolledrebar.
4) To determine an appropriate settings of cooling parameters for the rebar sizes studied.

1.5Research question

1) What is the chemical composition of the sampled billet used to produce the rebar?
2) What is the tensile strength of each rebar after altering cooling parameters?
3) What microstructures can be observed on each rebar after altering cooling parameters?
4) What is the appropriate cooling parameter settings for cooling the rebar?

1.6 Justification

The imbalanced setting of coolant temperature and coolant pressure compromises the quality of steel bars, owing to an average reject of 200 pieces of rebar in each production run. These cause a significant financial loss of Ugx. Shs.7,560,000,000 per annum and so this study helps to streamline the settings to achieve the desired quality and drastically reduce the financial losses.

1.7 Scope

The research concentrated on the effect of altering flow rate and coolant temperature on the tensile strength and microstructure of most commonly used steel bars for construction works (i.e. 12mm, 16mm & 20mm) that are produced from RRM Ltd, Namanve. The study was conducted from August to October 2018.

1.8 Significance of the Study

The study generated scientifically proven cooling parameter settings which helps to reduce production and financial losses of the company and implementation of the established settings would improve on the quality of the rebars and reduce collapse of structures like columns, beams, etc. in the community

1.9Limitations

i. Difficulty to conduct experiments on all data points due to calibration of the machines.
ii. It was difficult to obtain a temperature of 25℃ due to limitations of the cooling tower, so it was only possible to obtain 25℃ at the start of production when the coolant are at room temperature.
iii. Delayed data collection due tothe busy production schedule.

1.10Assumptions

I. Cooling taking place from the furnace outlet to the quenching zone inlet is negligible and constant for all rebar sizes under investigation.

II. Coolant sprays across the entire length of the rebar at a uniform temperature and flow rate.

III. The time spent by the rebar in the quenching zone is uniform for all the rebars under investigation.

CHAPTER TWO

LITERATURE REVIEW

This chapter presents the reviewed literature on heat treatment processes used in alteration of mechanical properties and microstructure of steel of different grades.

2.0Overview of Steel

Steel is basically alloys of iron and other elements in the periodic table. Steel is therefore defined as an alloy of iron, carbon (< 2% C) and other alloying elements that are capable of being hot and /or cold deformed into various shapes. The alloying elements include Fe, C, Mn, Si, P, S, Cr, Ni, Mo and other elements in various proportion, addition or removal of alloying elements in steel, will increase or reduce certain properties like hardness, ductility, malleability, forgeability, weld-ability,*(Huyett 2004).*Steels continue to gain wide use as prospective functional and structural materials in the rapidly developing industry because of their good soft-magnetic properties, high strength, good corrosion, and wear resistance coupled with relatively low material cost, *(Tokaji et.al, 2004;Martini et.al, 2004;Dearnley et.al, 2004 & Shi et.al, 1995).*

2.1 Classification of Steel

Steels are classified into two main groups, namely group one is is classified according to its application while group two is classified according to the composition of the alloying elements.

2.1.1 Classification of steel according to chemical composition

Developed nations like America, Britain, Japan, Korea and others have their own way of classifying steel while developing nations including most African countries have adopted the use of American and British way of classification and naming of steel. Steel has been classified by composition of the alloying elements and graded using a system devised byAmerican Iron and Steel Institute/ Society of Automotive Engineers (SAE/AISI),the four-or-five digit code designation of steel such as the nomenclature “AISI/ SAE1040 steel” means that the last two or

three digits, represents the carbon content and the first two digits represents the compositional class, thus the "10" represents the class of plain carbon steel and the "40" represents the carbon content of 0.40%, *(Ramio 2004).* The designation, grades, and composition runs into thousands, *(Merwin 2007).* as illustrated in Figure 2.1.

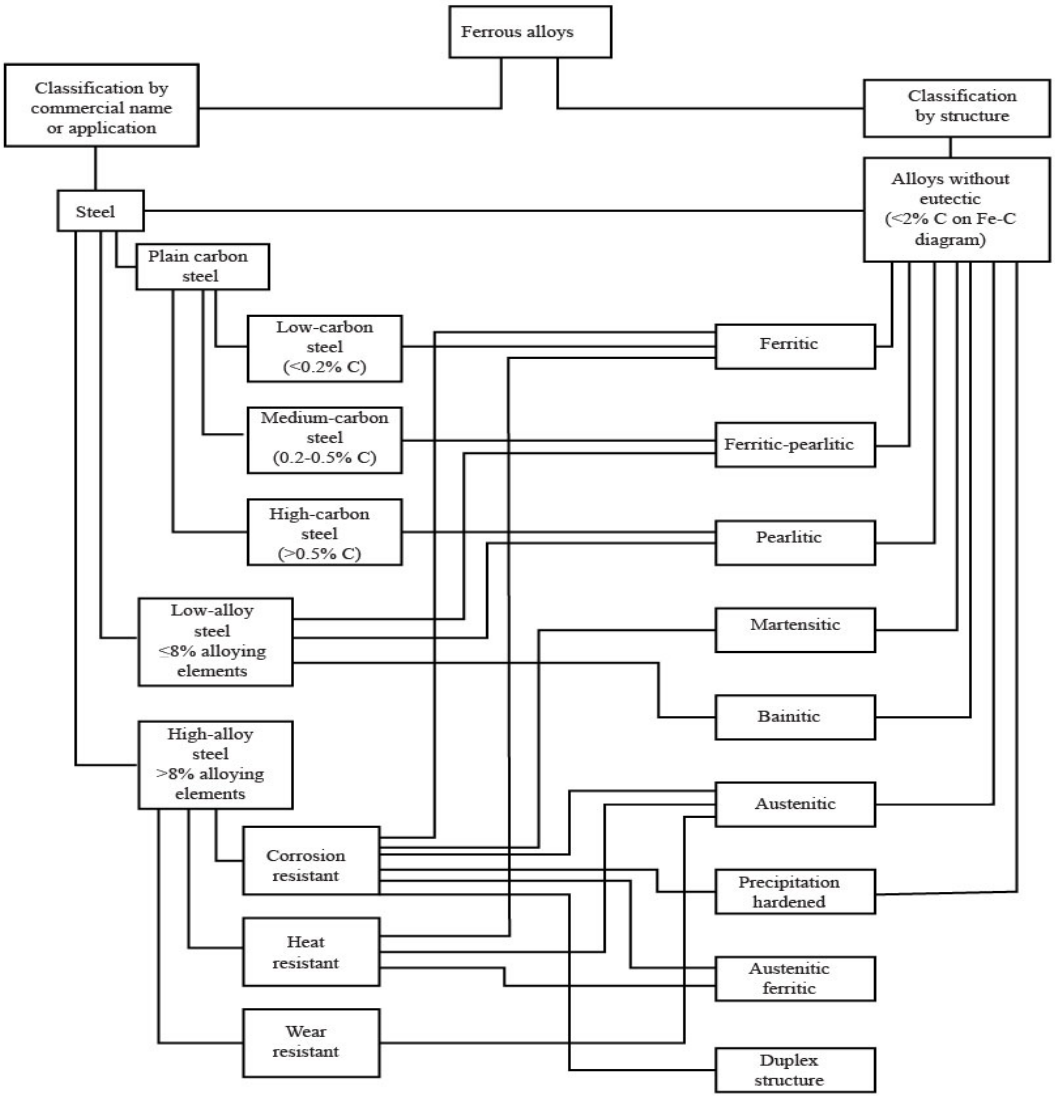

Figure 2.1: Classification chart for steels by chemical composition, *(Callister et.al, 2008)*

2.1.2 Classification of steel according to its application

The application of any steel material depends largely on its mechanical properties; coiled springs may require ductile steel while bridges may require hard steel, (*Ramio, 2004*). Steelsare designated according to their application and mechanical/physical strength such as 'S' Structural steel, 'P' steel for pressure purposes, 'L' steel for line pipes, 'E' Engineering steel, all these letters of alphabet are followed by a number being the specific yield strength in N/mm^2, others are 'B' steels for reinforcing concrete, 'Y' steel for pre-stressing concrete, and 'R' steel for or in the form of rail, all these letters are followed by a number being the characteristic yield strength and tensile strength respectively.

2.2 Chemical Composition of Steels

Steel consist of many alloying elements like Fe, C, Mn, Si, P, S, Cr, Ni, Mo and other elements Al, Bo, Pb, Ti, V, W, in various proportion, addition or removal of elements in steel, may yieldunique properties, *(Huyett, 2004).*The role played by different alloying elements is fairly complex. For instance, carbon is responsible for hardness and ductility when acting alone, however, in the presence of other elements such as manganese, silicon or oxygen, it is responsible for the formation of complex compounds like carbides with other elements, *(Drumond et.al, 2012).*

Plain carbon steels are categorized intothree groups, i.e. low carbon steel having a carbon content of < 0.2 wt. %, medium-carbon steels having a carbon contentbetween 0.2 to 0.5wt. %and high carbon steel having a carbon content of > 0.5 wt.% as illustrated in Figure 2.1**.** Low carbon steels having carbon content < 0.2 wt.%, are sometimes referred to as mild steel; the low carbon steels often have manganese content < 0.7 wt.%, with maximum values for silicon, phosphorus and sulphur at 0.6, 0.05 and 0.05 wt.% respectively *(Smith et.al, 2006).* The long service of low carbon steel and its performance depends on factors which include its grain size, its chemical composition, ultimate tensile strength, and amountof defects present as well as the operation condition employed on low carbon steel. Low carbon steels are utilized to produce cars body panels, tubes, domestic appliance side panels, and other engineering applications because they are readily available, workable and weldable, *(Fish, 1995).*

2.2.1 Effect of Carbon on the Strength of Steel

Carbon is the most essential element of all alloying elements in steel. Carbon controls the mechanical properties of steel due to its ability to lower the temperature of the phase change and creating new phases that do not exist in the iron itself.When the temperature of the phase change is lowered it facilitates rapid cooling, therefore, favoring the formation of martensite during the thermomechanical treatment process. Therefore the amount of carbon in steel affects the martensite hardness and hardenability,*(Valeria et.al, 2015).*This means that ductility will decrease with increase in carbon content, tensile strength increases with increase in martensite fraction while elongation to fracture decreases with increase in carbon content.

Carbon content is responsible for the attainment of different microstructures or crystalline structures with significantly different properties and the various thermal cycles that can exist during fabrication and heat treatment,*(Narayanasamy et.al, 2008)* furthermore carbon contenthasa specific effect on the tensile behavior and this result is in good agreement with *(Mead et.al, 1956), (Murata et.al,2000), (Chen et.al, 2001), (Yoo et.al,2005),* however, according to *Adnan et.al(2010),* the most distinctive aspect of strengthening of iron is the role of interstitial solutes, namely carbon and nitrogen.

Collinson et.al (1997) studied the effect of carbon on the stress-strain behavior of plain carbon steels for Zener-Hollomon conditions and found out that the carbon effect only appears in steels with >0.4% carbon and under high Zener-Hollomonconditions. Furthermore *Narayanasamy et.al (2008)* studied the effect of carbon content on stress ratio of steel. He found out that increasing carbon content of steel, the stress ratio,$\sigma_{true}/\sigma_{effective}$, andthe effective stress parameter is found to be higher compared to pure iron with no carbon content in powder metallurgy steels, where σ_{true}, is the axial stress and $\sigma_{effective}$, is the effective stress. On the other hand *Mead et.al (1956)* pointed out in his study that the carbon content does not only increase the self-diffusion coefficient of iron but also the activation energy for self-diffusion of iron decreases with increasing carbon content. Therefore, it is expected that the higher-carbon steels will have low activation energy for self-diffusion and increased self-diffusion coefficient of iron.

The ratio between yield strength and ultimate tensile strength at constant grain size is reduced with increasing carbon content, *(Pickering, 1978). Evans (1981)* studied AWS E7018-type electrode weld metal and found out that for C-Mn system, the best combination of tensile and

fracture properties is obtained with carbon content in the weld deposit in the range of 0.07% to 0.09%. Also *Surian et.al (1991)*studied the influence of carbon on mechanical properties and microstructure of weld metal from a high-strength SMA electrode and found out that an increase in the carbon content produces an increase in the amount of acicular ferrite at the expense of grain boundary ferrite.

2.3 Effects of other alloying elements on the strength of Steel

Silicon deoxidizes steel by dissolving in iron and removing bubbles of oxygen from the molten steel. This increases strength and hardness but to a lesser extent than manganese, but the resulting decrease in ductility could resent cracking problems, *(Drumond et.al, 2012).* Silicon normally appears in amounts less than 0.40 percent.

Manganese increases the rate of carbon penetration during carburizing and acts as a mild deoxidizing agent and responsible for taking the sulphur and oxygen out of the melt into the slag, however when too high carbon and too high manganese accompany each other, embrittlement sets in *(Leslie W.C. 1987).* Manganese combines with sulphur to form Manganese Sulphide (MnS), which is beneficial to machining however its ratio greatly affects weldability of steel. Manganese content of less than 0.30% promotes internal porosity and cracking in the weld bead, cracking can also result if the content is over 0.80%. the ratio of Mn:S should be 10 to 1. (Koyasu *et al. 1990)*

Phosphorus increases the hardenability of steel and is generally perceived as an embrittling element in steel due to its segregation tendency to grain boundaries (*Grabke H.J. 1987),* the presence of phosphorus in steel increases its corrosion resistance in coastal region*, (Kreyser G. and R. Eckermann, 1992)*

Aluminium addition in steel leads to a certain decline of tensile strength, the yield strength and elongation are neither decreasing significantly, especially the former is improved after heat treatment (*Haifeng XU et.al,2015).*

Copper has a small impact on hardenabilityand it increases the corrosion resistance of steel due to the formation of a very thin oxide film on the steel surface, its amount in steel is not less than 0.20 percent (*Yamashita .M et al, 1998),* (*Schwabe .K 1971).*

Witmer D.A and Willison R.M (1970), showed that increasing the nitrogen during steelmaking markedly increases hardness and yield strength and decreases the tensile elongation, whereas even larger amounts of nitrogen absorbed during annealing have a much smaller effect on these properties.

2.3 Mechanical Properties of Steel

High strength requirement of Thermo-mechanically treated (TMT) rebars is crucial in many engineering application due to its good combination of the mechanical propertiesespecially in the construction of bridges, buildings, fabrication works, etc. According to the Uganda Standard and the East African Standard (US-EAS 412-2:2013), the yield strength of hot-rolled rebar is expected to be between 450MPa and 550MPa, depending on prescribed standards and application.

Manojkumar et.al (2012) studied the improvement in yield strength of deformed steel bar by quenching using Taguchi Method and the experiment was aimed at optimizing the effects of process parameters such as water pressure, speed of bar, cooling rate and Temperature of bar on the yield strength, results revealed that water pressure and cooling rate have a significant effect on yield strength at a confidence level 95 %. However, water pressure has the most significant effect on yield strength as shown by much higher F-ratio (*i.e.* 90.82) and also percent contribution (*i.e.*65.24).

Musonda(2017) studied the effect of water flow rate on the yield strength of a reinforced bar and found out that the flow rate, became stable from 619 to 645m^3/ h after several adjustments made to flow rate and the yield stress remained stable and maintained between 482 Mpa to 530 Mpa.The design tensile and yield strengths of SA 178 GrA Carbon steel typically decreased from172.25 Mpa to 158.47 Mpa with an increase in temperature from 37.8^{0}C to 93.3^{0}C as shown in Figure 2-2. According to *Musonda (2017)* this reduction follows the same trend for SA 516 Gr 55 and SA 515 Gr 70 carbon steels. It should be noted that this is not, in fact, the actual behavior of the carbon steel because the actual tensile strength might decrease slightly and then increase

due to strain aging. The design values are modified so that the design tensile strength is not allowed to increase with temperature.

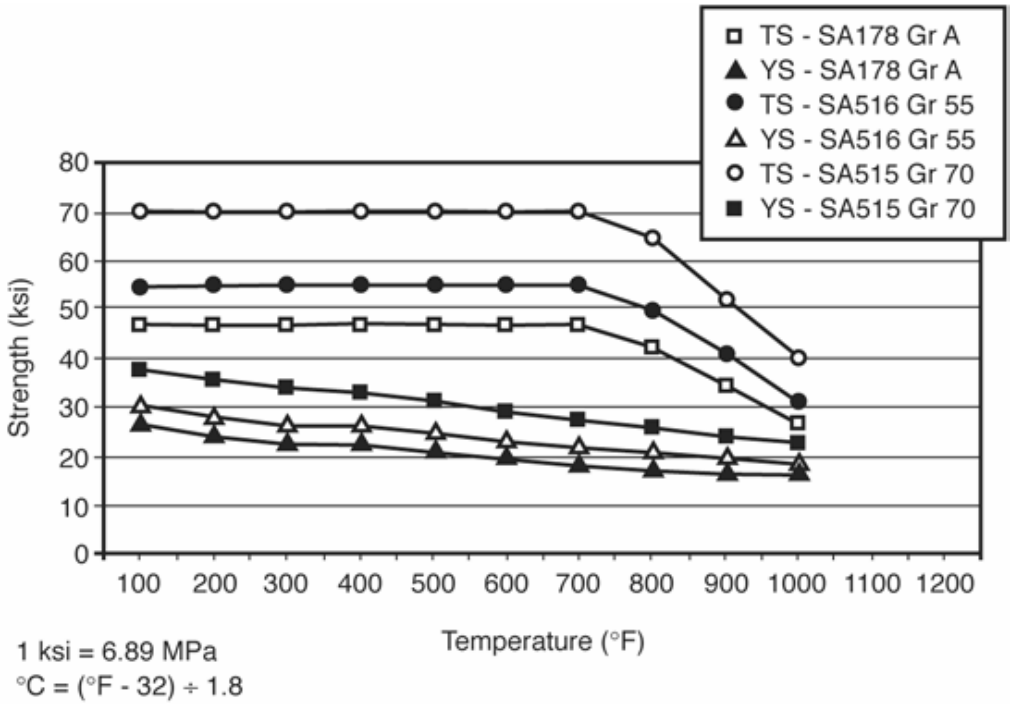

Figure 2.2: Design Tensile and YS of Carbon Steels versus Temperature (*Musonda, 2017).*

Merwin(2007), reportedthatmedium manganese steels having a combination of 0.1C–5Mn, 0.0095C–5.8Mn and 0.099C–7.09Mn,had combination of high strength ranging between 800–1000 Mpa and total elongation between 30–40%, this implies that a combination of manganese and carbon can be used to produce steel of high strength which is applicable for vast engineering worksthat requirea mixture of high strength and ductility.

Yi (2011), found out that ferrite/austenite duplex C–Mn steels (named -TRIP steel), had ultimate strength of 900Mpa and total elongation 28%**,** this result displays that ferrite/austenite duplex C–Mn steels offer a better strength with less ductility which disapproves the findings of*(Merwin, 2007).*

Another type of C–Mn steels developed by Central Iron and Steel Research Institute in 2013, having Mn between 3 and 9 wt.%,was capable of producing substantially improved mechanical properties with high strength between 1–1.5GPa and high elongation between 30 - 40%, which

was processed by ART-annealing with relative long time to develop ultrafine austenite and ferrite duplex structure with austenite fraction about 30–40%.

The trend of results by earlier researchers showed increased strength and high percentage elongation meaning that there is possibility of inventing more types of C–Mn steels with more percentage composition of medium manganese to produce higher strength than what has been attained by *(Merwin, 2007;Central Iron and Steel Research Institute, 2013;Shi et.al, 2010; Wang et.al, 2011; Xu et.al,2012).*

2.3.1 Mechanical behavior of Fe-C alloys

The strength and hardness of the different microstructures are inversely related to the size of the microstructures (fine structures have more phase boundaries inhibiting dislocation motion). The strength of martensite is not related to microstructure. Rather, it is related to the interstitial carbon atoms hindering dislocation motion and to the small number of slip systems *(Pickering, 1978)*

Cementite is harder and more brittle than ferrite - increasing cementite fraction, therefore, makes harder, less ductile material, spheroidite is the softest, Fine pearlite is harder and stronger than coarse pearlite and Bainite is harder and stronger than pearlite, therefore, Martensite is the hardest, strongest and the most brittle of all the various microstructures in steel alloys as illustrated in Figure 2.3 and Figure 2.4*(Pickering, 1978)*

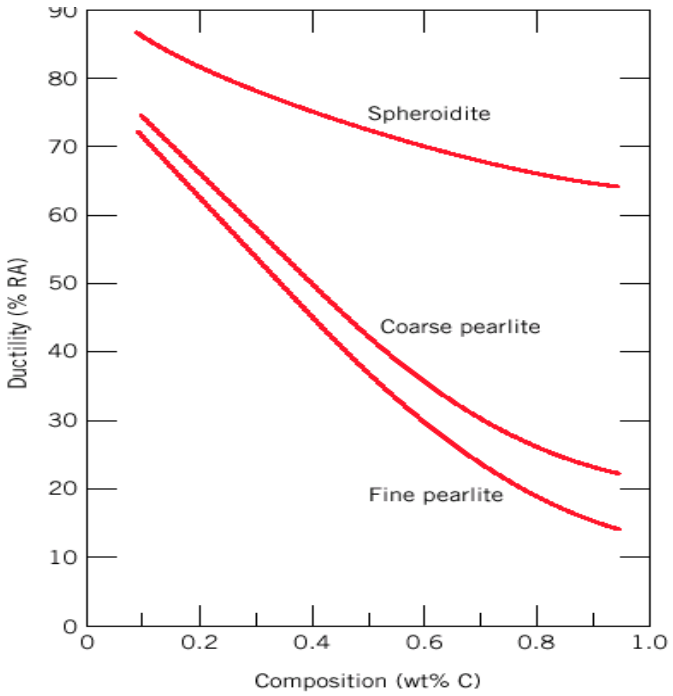

Figure 2.3. Ductility of different grade of pearlite versus composition *(Pickering, 1978)*

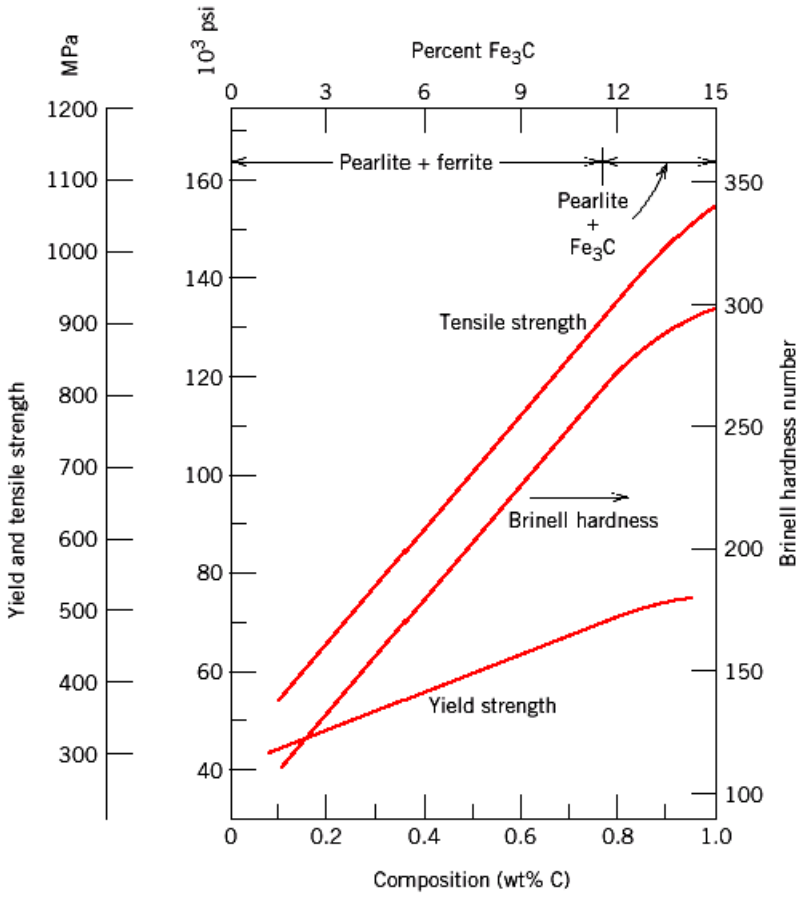

Figure 2.4: Strengths and hardness versus composition,*(Pickering, 1978).*

2.4 Microstructure of Steel

The microstructure is the structure of a metal as revealed by microscopic examination of the etched surface of a polished specimen. Metallic materials take the form of a crystalline structure in the solid state with the exception of amorphous metals formed under radical cooling conditions.

The crystalline structure and the alloying elements added to pure iron increases the ability of carbon steel to have a wide range of properties which makes it one of the most useful materials in the industry today. The crystalline structure of carbon steel might include body-centered cubic (ferrite), face-centered cubic (austenite), or body-centered tetragonal (martensite) forms *(Park, 2004).*

The crystalline structure forms in many directions during solidification from the molten state of the material,solidification starts from initiation points and continues until the crystalline structure that is formed runs into another island that started from a different point *(Park, 2004).*

Each of these islands of a single orientation is a grain that exists as a singular structure. The size of these grains also contributes to the properties of the material, also affects the ability of the material to form certain microstructures and as the material cools, carbon steel crystalline structures are forced to change from one structure to another in a process called phasetrans formations, *(Park, 2004).*

The different structures have different limits of solubility of the alloying elements, primarily carbon in carbon steels, the microstructure can also contain other compounds, such as metallic carbides, interspersed with the crystalline form. The complex microstructure of carbon steel includes the crystalline structure, the grain size and frequency of the interspersed metallic compounds.

Carbon steels can exist in different microstructures or combinations of microstructures. The microstructures of carbon steels include not only the crystalline structure but also various metallic carbides or compounds in different arrangements. Pearlite, upper bainite, and lower bainite are examples of the arrangements that can exist,*(Leslie, 1987).*

The standard metallurgical atlas used in this study described Pearliteas an arrangement of thin alternating and roughly parallel lamellar platelets of ferritic (body-centered cubic) structures with iron carbides (Fe_3C) called cementite which can have a coarse or fine structure but are often recognizable with optical microscopy and Bainiteas an arrangement of aggregates of ferrite with distributions of precipitated carbide particles *(Leslie, 1987)*

However, the arrangement of the aggregates can take different forms which culminate to terms like upper Bainiteand lower Bainite. Upper Bainiteconsists of small ferrite grains that form in plate-shaped sheaths. These grains are interspersed with the cementite that forms at relatively high temperatures. Lower Bainite consists of needlelike ferrite plates containing a dispersion of very small carbide particles as shown in Figure 2.3 *Park (2004).*

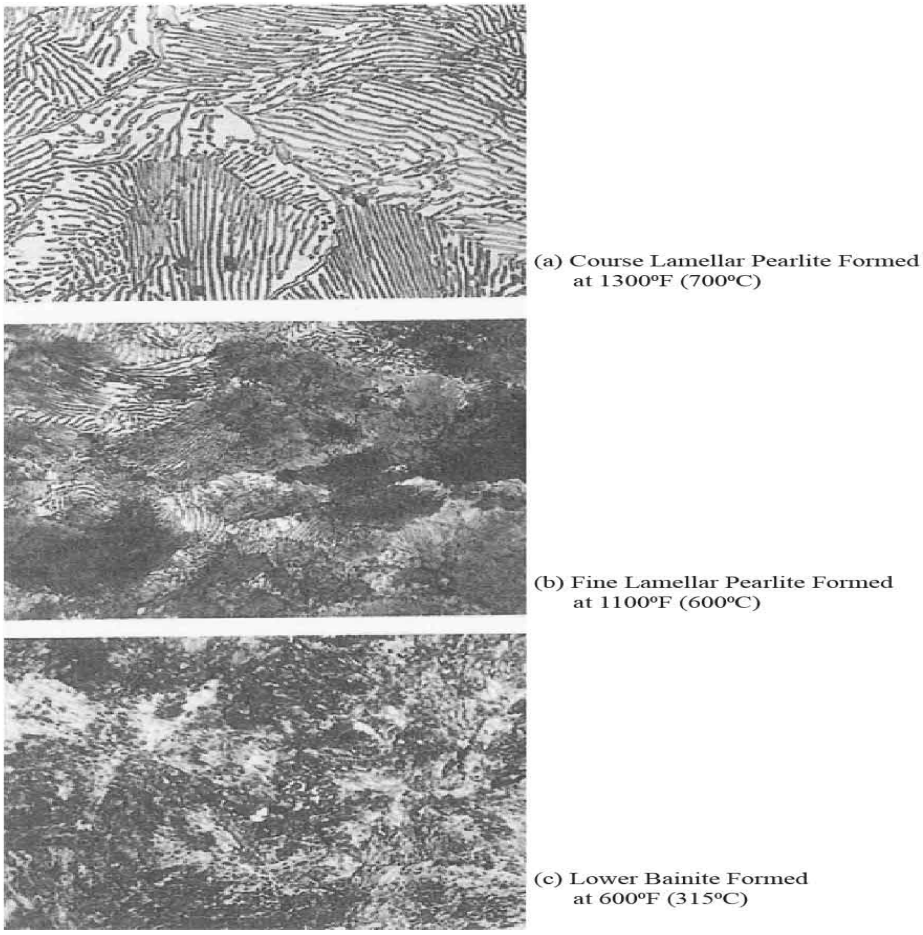

Figure 2.5: High Carbon Steel Microstructures (0.77% C), Mag. X500, *(Flenner, 2007).*

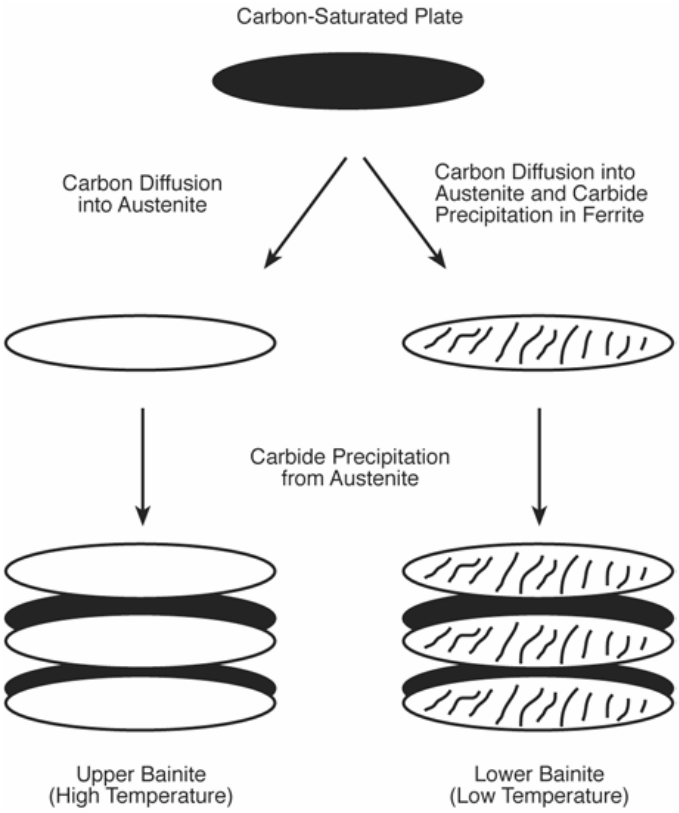

Figure 2.6: The Growth and Development of Bainite Morphologies*, Park (2004).*

2.4.1 Microstructural transformation of steel

The ferritic structure at room temperature known as alpha (α) ferrite,has a relatively low ability (< 0.008%) to contain carbon atoms in the space between the iron atoms (interstitially), this results into few carbon atoms in the structure hence responsible for high ductility and softness.

At higher temperatures, the ferritic structure becomes unstable and transforms into a face-centered cubic structure called gamma (γ) austenite which has a much higher affinity for carbon and can contain as much as approximately 2.1%, this percentage of carbon that cannot be contained interstitially is responsible for the strength of steel. At even much higher temperatures, the austenitic structure transforms into a higher temperature form of ferrite known as delta (δ) ferrite,*Flenner (2007).*In a carbon steel microstructure, iron carbides can appear as platelets or particles of cementite (Fe_3C). A microstructure that has alternating platelets of ferrite and cementite is called pearlite.

Iron-iron carbide phase diagram shown in Figure 2.6 represent the crystalline structures, or phases, of the carbon steels in an equilibrium state that are determined by very slow cooling from molten material. This effect can be seen in the temperature difference between A1, the equilibrium lower transformation temperature and Ar1, the lower transformation temperature upon cooling. Although not shown, there is also a lower transformation temperature upon heating, Ac1, which is somewhat higher than A1. The Ac1 temperatures depict the start point of the transformation between the α ferrite and the γ austenite upon heating, *(Flenner, 2007).*

The phase diagram in Figure 2.6, also shows an equilibrium upper transformation temperature A3. Similar to the variations noted for A1, there are also upper transformation temperatures upon heating and cooling (Ac3 and Ar3, respectively). The transformation temperatures indicate the points at which the structure becomes an unstable form and begins to under go a transformation to a different crystalline structure.

It can be seen that carbon steels, with a typical maximum carbon content of less than 0.35% for pressure-containing applications, will have a transformation temperature range that will vary with the carbon content and the rate of heating or cooling. The explanations of microstructure transformation by *Flenner (2007)* agrees with, *Leslie (1987).*

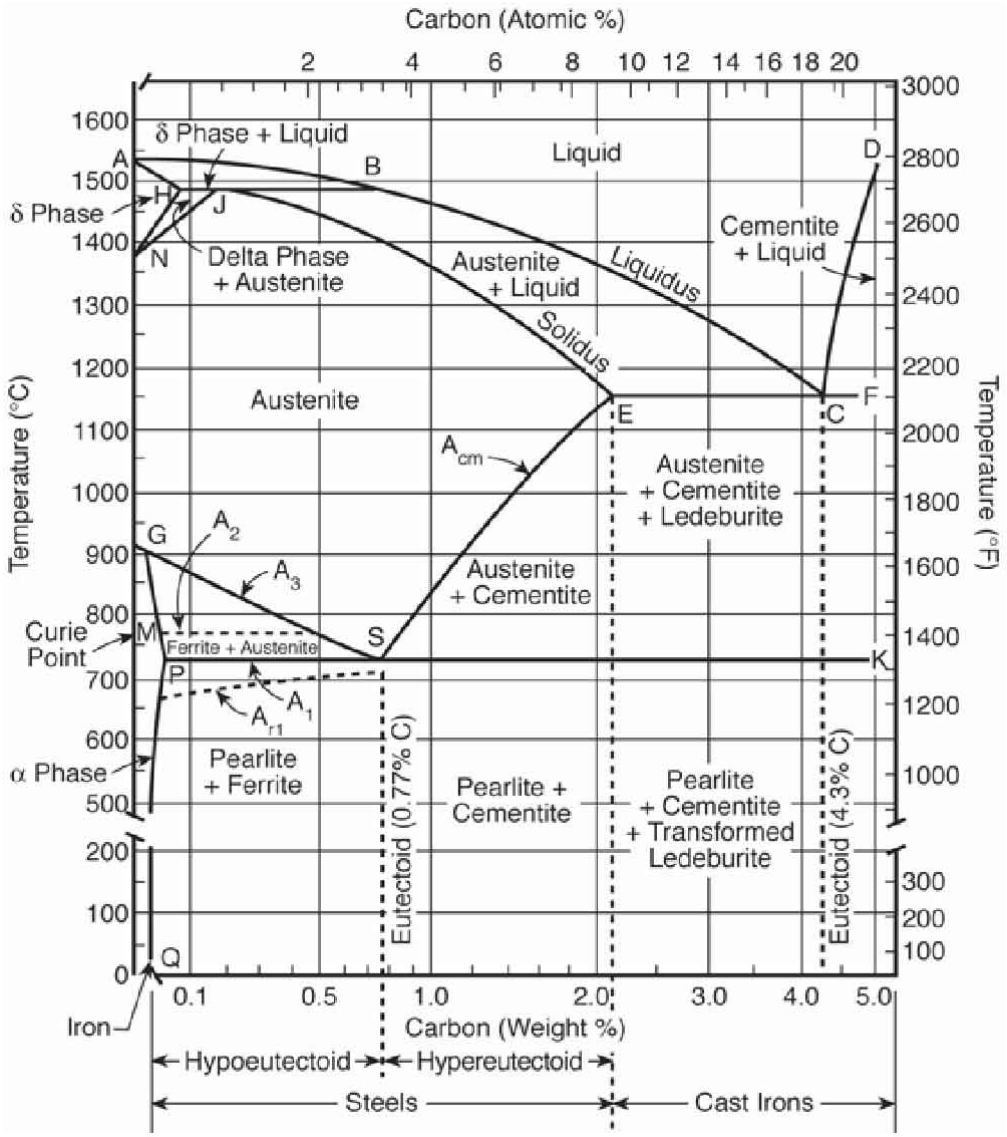

Figure 2.7: Iron-Iron Carbide Phase Diagram*, (Flenner, 2007).*

2.5 Heat Treatment of Steel Bars During Production

The production process involves melting scrap metals to form billets, having the required chemical composition and extruding it through a die into the quenching zone. Just like water, steel undergoes phase changes from liquid-austenite-ferrite and these involve heating the material to austenitizing temperature, followed by rapid cooling in the TMT box where the last phase can be developed. The quality of the last phase depends largely on the cooling parameters like coolant temperature, quenching time, type of coolant, and diameter of the product, (*Huyett, 2004).*

Heat treatment is highly dependent on the manufacturing methods used for a particular product, the forms of heat treatment include quench hardening, annealing, or normalizing that might be followed by tempering heat treatment. Engineering materials, mostly steel are heat treated under a controlled sequence of heating and cooling to alter their physical and mechanical properties in order to meet the desired engineering applications. The effect of heat on steel allows for the growth of grains in the microstructure making it soft and ductile. On cooling the micro grain structure settles to martensite, pearlite, and ferrite depending on the rate of cooling.

The effect of heat treatment on the microstructure has been studied by many researchers including *(Fadare et.al, 2011), (Huyett,2004)* and their results showed that the mechanical properties of steel can be changed and improved by various heat treatments for a particular application.Prior to *Fadare(2011), Alwandayi (2009)*had studied the impact of partial heat treatment on mechanical properties of solid high-carbon steel used in manufacturing active parts of cold cutting templates, the results were that high strength between 800 Mpa to 900 Mpa was registered and used as a cutting template during manufacturing.

2.5.1 Rapid quench heat treatment

If the cooling rate is too rapid to allow nucleation and growth mechanisms (also called critical cooling rate), the result is that the trapped carbon is forced into the crystalline lattice and instead of forming ferrite structures, the austenite lattice shears and results in a body-centered tetragonal structure called martensite shown in Figure 2.8 *(Park 2004)*,.The martensitic transformation occurs without diffusion of the carbon and therefore occurs very rapidly. In addition, once the austenitic structure is undercooled to the point at which the carbon cannot diffuse and additional ferrite cannot form, the only remaining transformation that can occur upon further cooling is to martensite.

The temperature at which martensite begins to form from austenite is the *Ms.* Because ferrite cannot form, martensite will continue to form as the temperature decreases from any existing austenite until all of the austenite is transformed, which occurs at the martensite finish temperature, or *Mf*. This carbon steel martensitic structure is known to be both hard and strong but lacks ductility and toughness in the un-tempered state. The resulting maximum hardness is closely related to the carbon content of the steel and the percentage of martensite that is formed.

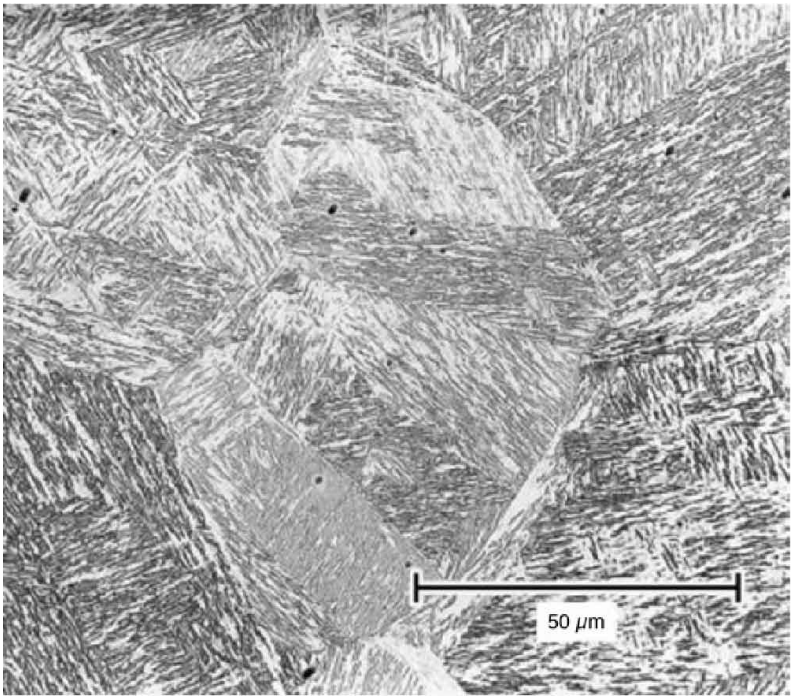

Figure 2.8: Microstructure of Water-Quenched Low-Alloy Steel,Mag. X500*(Park,2004).*

2.5.2 Tempering heat treatment

Tempering is normally done at temperatures between 350°F and 1300°F (175°C and 705°C) from 30 minutes to 4 hours,this allows some of the carbon atoms in the strained martensitic structure to diffuse and form iron carbides or cementite, an increase in the temperature of steel during tempering lowers the yield strength, tensile strength, hardness, and thus relieves some of the stresses but increases ductility and toughness, *(Leslie, 1987).*

Fadare et.al (2011) alternately heat-treated Steel specimen as: Annealing, oil quenching, and tempering at 200^0 C, 400^0 C and 600^0 C for around 1hr respectively, the conclusion after testing the specimen at room temperature was that increasing the tempering temperature decreases the hardness of steel, also increasing the tempering temperature increases the ductility of the steel, although steel with copper has low ductility as compared to steel without copper.

Martensite is so brittle and unfit for engineering applications, so tempering allows the transformation of martensite to pearlite and ferrite enabling it to be fit for most engineering application, *(Shizhong et.al 2006).* There are a number of microstructural changes that take place during tempering heat treatment due to the effect of tempering temperature, these structural

changes includethe isothermal transformation of retained austenite precipitation of carbon from a body-centered tetragonal lattice of martensite, growth, and spheroidization of carbide particles and formation of ferrite-carbide mixture makes tempered martensite less hard/strong as compared to regular martensite which has enhanced ductility, *(Rajan et.al 1994).*

The mechanical properties depend upon cementite particle size, therefore fewer and larger particles mean less boundary area and softer, more ductile material eventual limit is spheroidite. Particle size increases with higher tempering temperature and/or a longer time, hence making the material softer and more ductile, *(Shizhong et.al 2006).*

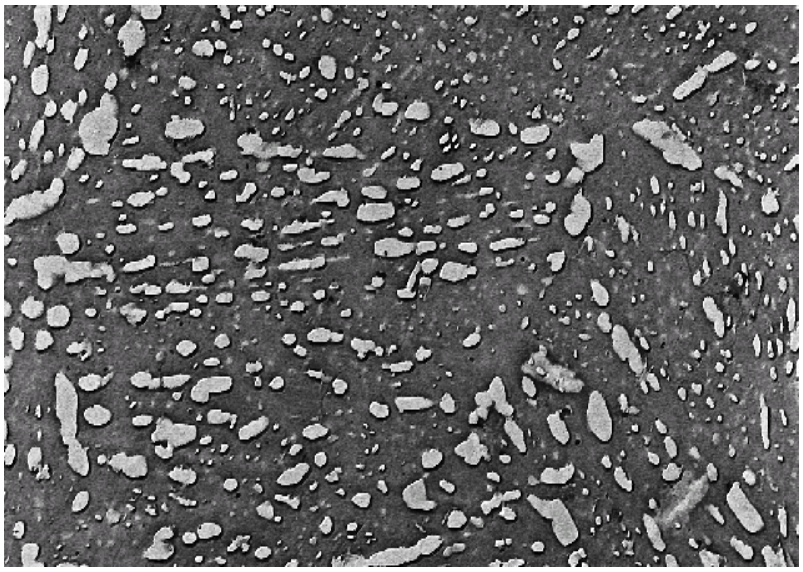

Figure 2.9: Electron micrograph of tempered martensite *(Totten et.al 1993).*

The properties of steel that have been quenched and then tempered depends largely on the rate of cooling, tempering time and tempering temperatures, *(Shizhong et.al 2006).* Holding temperature between 850^0C to 1150^0C and increasing holding time result in an increase in grain size as shown in Figure 2.9 *(Totten et.al 1993).*

Much as *Totten et.al (1993), Shizhong et.al (2006)* tackled the effect of increasing holding temperature and cooling rate on steel, they did not extend it to tackle the effect of altering the size of the specimen and temperature of the cooling medium on the mechanical properties of steel.

2.6Effect of Cooling Parameters on Heat Treated Rebar

For a given operation condition, the temperature and its distribution within the bar entering into the quenching chamber playsa crucial role in controlling the mechanical properties of rebar such as yield strength, percentage elongation, and ultimate tensile strength. Therefore understanding the entire cooling system is essential to gain a better insight into what happens during the cooling process. Furthermore, the controllability of the cooling process is the most important aspect for achieving the required mechanical properties.

Parameters such as the type of nozzle, spray distance, water impingement density, nozzle position, nozzle overlap, movement velocity, and scales have significant influences on the cooling intensity *(Chabicovsky et.al 2013, Raudensky et.al (2014), Chabicovsky et.al (2015).*The length of the quenching chamber and the cooling water flow rate are the obvious control variables because they are easy to adjust during hot rolling and they have a strong effect on the yield strength of the rebar *(Simon et.al 2017).*

Depending on the chemical compositions of hot-rolled rebar, cooling parameters might be adjusted for optimization of mechanical properties of the rebar *(Kabir et.al 2014).* However, the possible problems encountered in TMT of rebar may include low quenching rate or longer period of time spent by the hot rebar in the quenching chamber which will definitely affect the mechanical properties of steel on cooling, the transition zone of steel is highly affected, this usually results in a larger area of transition zone of steel *(Kabir et.al 2014).*

The imbalanced cooling will result in insufficient inner heat of the rebar core which may not be able to temper the martensite case properly. The result is that the case area will be either very soft or hard. For soft case, the steelwill not provide optimum design strength and for a very hard case, the steel will not provide optimum ductility which might cause brittle type of failure, therefore it should be noted that control of the cooling rate of the surface area of rebar is very important in controlling the mechanical properties of rebars.

As a standard practice, the surface temperature should be cooled to below 200 ℃ at the cooling bed and this should be done within a few seconds,*(Kabir et.al 2014).*In the absence of online temperature tracking, a pyrometer or an Infrared Thermometer (IR) can be used to monitor this temperature at the cooling bed. The temperature at the cooling bed eventually settles to room

temperature. It is at the cooling bed where mechanical properties of rebar arefinalized to obtain the desired fine grain sized ferrite. Despite the above, *Kabir et.al (2014)* did not study the effect of flow rate on strength of different rebar sizes.

Fink & Willey(1948) described the relationship between cooling rate and the final alloy strength by identifying the temperature range over which the cooling rate has its most critical influence on the mechanical properties of the aged material. Their research resulted in the development of the C-curve which represents the critical time required at different temperatures to precipitate a sufficient amount of solute (alloying elements) to reduce the maximum strength or hardness by the percentage represented by that particular curve.

2.6.1 Effect of temperature on strength of steel

When steel is heated to a higher temperature, a lot of microstructural transformation takes place *(Flenner, 2007)*.Figure 2.10,illustrates how the micro grain structure grows depending on the amount of heat applied and the material become so ductile, heating the carbon steel microstructure through the transformation range, the ferrite will transform into an austenitic structure, because the austenitic structure has a much higher solubility of carbon, the iron carbides dissolve and the carbon enters into solution with the austenitic iron microstructure.

This is a time and temperature dependent mechanism that takes longer if the cementite particles or platelets are large. An increased rate of heating will have the effect of requiring a higher temperature to complete the dissolution as illustrated by *Flenner (2007)*in Figure 2.10**.**

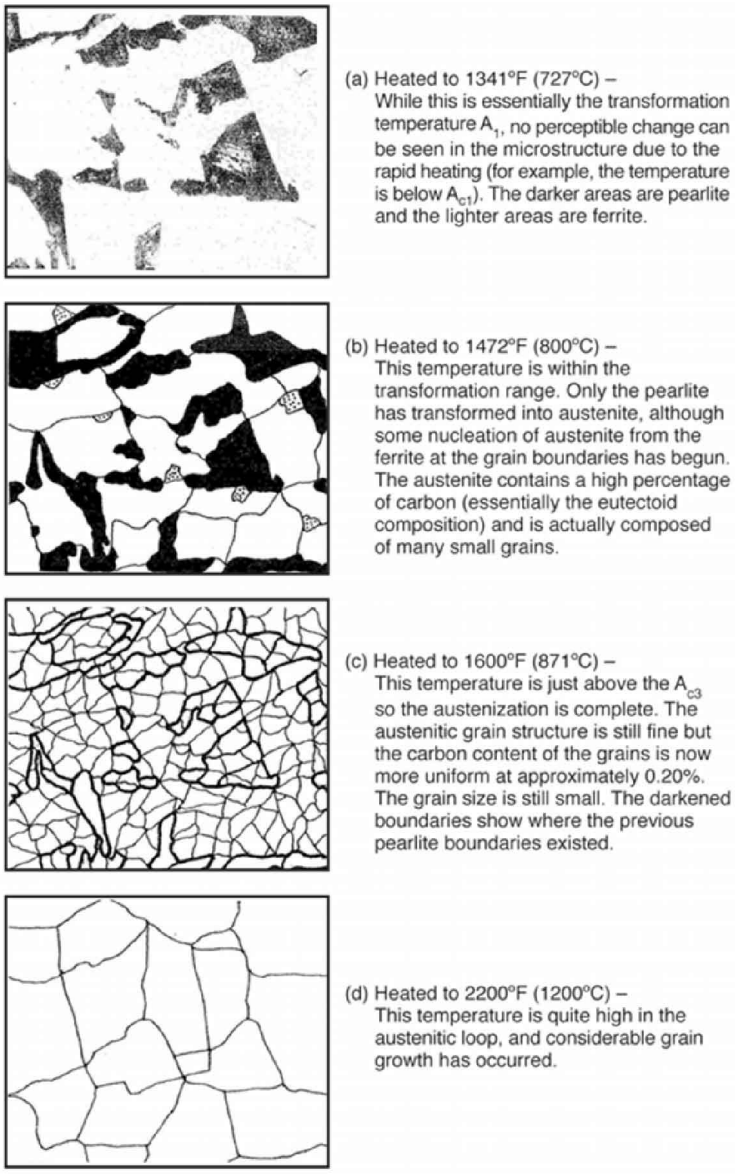

Figure 2.10: Illustration of grain growth of plain carbon steel (0.20% C),*(Flenner, 2007).*

The grain size becomes quite small when full austenitization has taken place and upon reaching the temperature slightly above the upper transformation temperature Ac3 but upon subsequentcooling, the fine grain structure becomes essentially maintained. However, larger grain size is achieved if the metal is heated to a higher temperature before cooling and the result is a coarse grain structure in the room temperature structure. The temperature reached during thermal cyclesupon heating above the transformation temperatures will, therefore, have a significant effect on the endproperties of the material.

When austenitized carbon steel is cooled very slowlyand ferrite grains begin to form just below theAr3 (the upper transformation temperature upon cooling). These ferritegrains cannot contain the typical carbon content levels of carbon steel and as a result, the content increases in the austenite grains which is exactly the reverse of what happens when the ferritic grains are heated through the transformationtemperatures shown in Figure 2.3.

As the material is cooledfurther toward the Ar1 (the lower transformation temperature upon cooling), more ferrite is formed at the grain boundaries of the austenite,and the austenite continues to gain carbon content and these will continue until the Ar1 temperature is reached, at which point the austenite can contain as much as about 0.77% carbon, *(Park, 2004).* This isillustrated in Figure 2.11, from point c down to point d justabove the Ar1 temperature (marked as 723ºC).

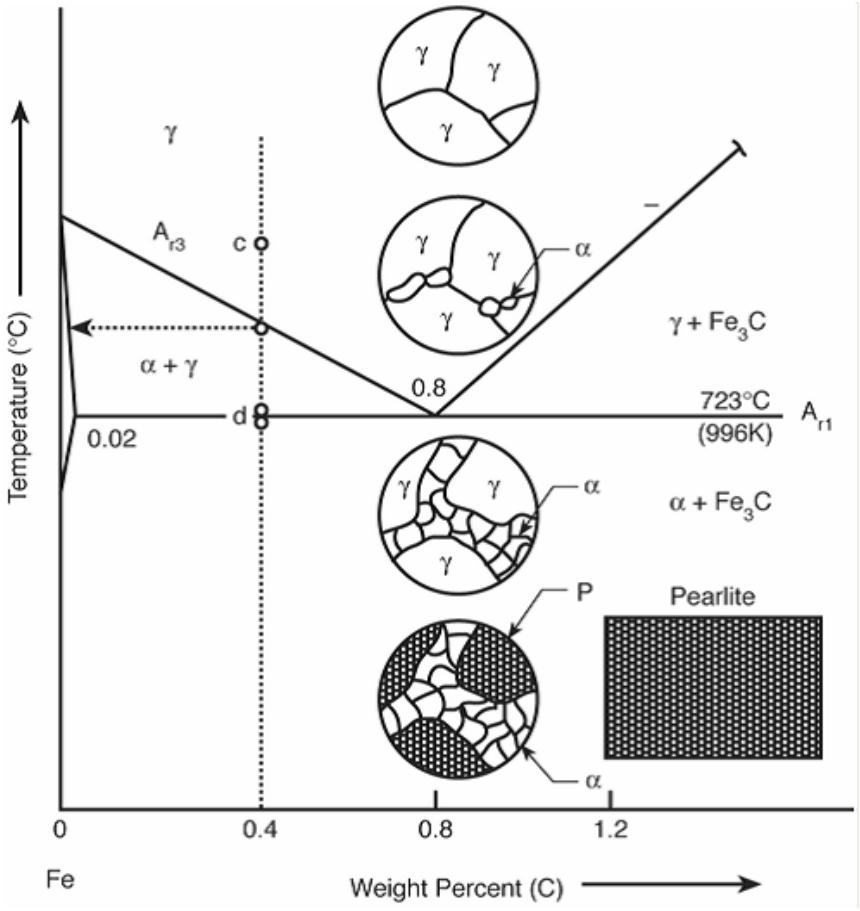

Figure 2.11: Transformation of Carbon Steel withSlow Cooling,*(Park, 2004).*

When the structure cools further to just below the Ar1 temperature (as represented by point d just below Ar1 in Figure 2.11,the high-carbon austenite transforms to ferrite and cementite, the ferrite becomesunable to accommodate high carbon content hence facilitating the formation of pearlitic microstructure in which the ferrite and the cementite are arranged in alternating lamellar platelets.

The formation of ferrite and pearlite from austenite is a nucleation and growth mechanism therefore slow cooling gives adequate time for nucleation and growth mechanism to occur but as the cooling rate increases, the austenite is undercooled to a temperature below the Ar1 (lower transformation temperature), owing to microstructural changes in the material.

When cooling of steel takes place in equilibrium condition, the structure of carbon steel results in a ferritic structure with grains of pearlite. In this case, the carbon in the austenite has the time to diffuse into the cementite platelets and allow the ferrite platelets to form. The result is coarse pearlite with ferrite grains that formed at the grain boundaries but if the austenite is undercooled slightly before transformation can occur, the result is a finer pearlitic structure because the time for the carbon to diffuse into the cementite platelets is shortened. Also, the nodules of pearlite and the grains of ferrite tend to be smaller and as a result strength and hardness are increased *(Park, 2004).*

Bainitic structures occur when the undercooling of the austenite is such that pearlite can no longer form and the formation of martensite has not yet started (that is, the martensite start temperature [Ms] has not been reached). Bainite can take different morphologies (patterns) as either upper bainite Figure 2.12**,** or lower bainite Figure 2.13, depending on the temperature at which it forms. Upper bainite will be somewhat harder and tougher than the pearlite if it forms. Lower bainite will not be as hard as martensite but can be much tougher, *(Park, 2004).*

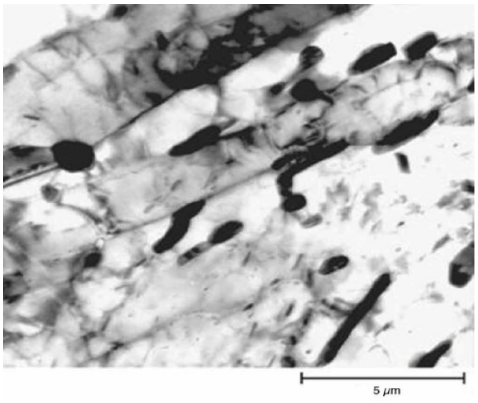

Figure 2.12: Microstructure of Upper Bainite as Seen in the TEM Mag.X5500, *(Park,2004)*

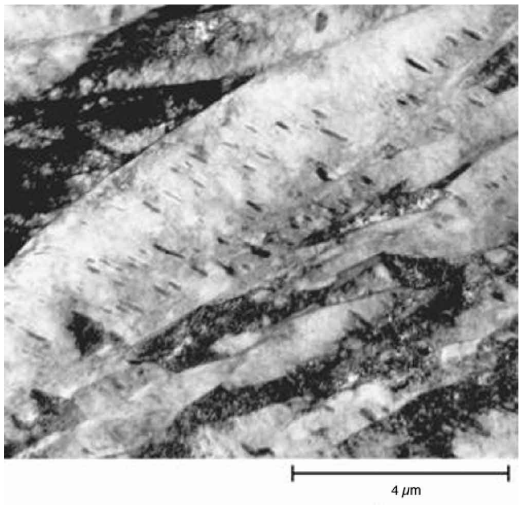

Figure 2.13: Microstructure of Lower Bainite, viewed using TEM Mag. X8000, *(Park,2004)*

2.7 Spray quenching of the rebar

Spray quenching enhances the temporal and spatial heat treatment possibilities, the parts can be cooled by arrays of individually configured high-pressure water sprays upon exiting the extrusion die, *(Schöne, 2012).*Spray quenching has emerged as the quenching method of choice, unlike bath quenching, the part can be cooled by arrays of individually configured high-pressure water sprays upon exiting the extrusion die and down-sizing rollers, *(Toda, 1972).*

A spray consists of a multitude of droplets with controlled sizes, speeds, and trajectories, and is popular in many cooling applications, *(Lefebvre, 1989).* Aspray is obtained through the atomization of a liquid by pressurized gas in a specifically shaped nozzle and the primary cooling advantages of sprays compared to competing for cooling schemes are their ability to

increase heat transfer effectiveness and spread the cooling over a broad surface area, *(Schöne, 2012).*

The method used for cooling hot rebar, type of coolant used, coolant temperature and cooling time during quenching can be altered and results in different mechanical properties and microstructures of steel, *(Huyett, 2004).* Spray quenching offer a wide range of heat transfer coefficients in comparison to other quenching methods, *(Deiters et.al, 1989;Schöne, 2012;Pola et.al, 2013).*

Spray cooling allows the cooling rate to be controlled by adjusting the nozzle sizes, spray distance, volumetric flux, Sauter mean diameter, and mean drop velocity whereas bath quenching offers no control, since the entire part is constantly in contact with the coolant, the spray parameters that have the strongest influence on cooling performance are volumetric flux, Sauter mean diameter, and mean drop velocity *(Toda, 1972 Mudawar et.al, 1989; Deiters et.al, 1990; Klinzing et.al, 1992; Hall, 1993; Totten et.al,1993; Hall et.al, 1995; Estes et.al, 1995; Mudawar et.al, 1996; Hall et.al, 1997; Chen et.al, 2002; Rybicki et.al, 2006).*

2.7.1 Effect ofspray quenching on strength of rebar

Rapid quenching suppresses precipitation but can lead to large spatial temperature gradients in complex-shaped parts causing distortion, cracking, high residual stresses, and/or non-uniform mechanical properties, conversely, slow cooling significantly reduces or eliminates these undesirable conditions but allows considerable precipitation, resulting in low strength, soft spots, *(Hall et.al, 1997)*.

Joseph et.al, (2015) studied the effect of velocity of impact on mechanical properties and microstructure of mediumcarbon steel during quenching operations and found out that the cooling rates exhibited significant dependence on velocity of impact with the general trend showing increased cooling as velocity of impact is increased, as the velocity of impact increases, the maximum cooling rate also increases and the hardness and ultimate tensile strength also increases.

Coolant additives and surface augmentation techniques are commonly used to enhance the rate of heat removal, *(Thome,1990, Xuan et.al,2000, Honda et.al,2002 Ujereh et.al,2007).*

Hall et.al,(1996) developed a CAD/CAM system able to run boiling and two-phase flow laboratory which would facilitate on-site control of the quenching process. He performed experiments in which the initial nozzle configuration was selected based on thermal mass distribution of the extrusion and the result was, improved subsequent quenches by increasing the cooling rate of the slowest-cooling regions of the extrusion or decreasing the cooling rate of the fastest-cooling region such that the magnitude and uniformity of hardness and yield strength was maximized while maintaining relatively low spatial temperature gradient (i.e. low residual stress).

The technical challenge of quenching is to select the quenching medium and process that will minimize the various stresses that develop within the part to reduce cracking and distortion, while at the same time providing heat transfer rates sufficient to yield the desired as-quenched properties, *(Hassan et.al, 2010)***.** But achieving desired mechanical properties and minimizing the possibility of occurrence of quenching cracks are the key indicators of the successful hardening process. Apart from the hardenability of the alloy, the geometry of the part, and the coolant used, the effectiveness of quenching depends on a number of other external factors such as temperature, agitation and volume of the coolant, *(Totten et.al,1993).*

Agitation or forced circulation of the coolant during quenching generally enhances heat transfer at all stages of cooling, *(Fernandes et.al,2007).* Without agitation, heat flow through the film boundary at the surface of the part is reduced and obtaining a forced convention fluid regime reduces the resistance to heat flow at the fluid film boundary layer*(Fadare et.al,2011).* This can be achieved by mechanically moving the parts through the bath, pumping to re-circulate the coolant or mechanically inducing agitation circulation of the fluid, *(Mohammed, 2010).*

Agitation affects the hardness and depth of hardening during quenching because of the early breakdown of the vapor blanket which results in the nucleate boiling, this process results in a time reduction of the slow cooling stage thus resulting in rapid heat transfer, *(Alberg, 2003; Bohumil et.al, 2012).*

CHAPTER THREE

METHODOLOGY

This chapter presents the methods employed in investigating the effects of process parameters in alteration of the tensile strength of hot-rolled steel bars. The investigation procedures, equipment used, materials and data analysis techniques are explained.

3.1 Research Design

Quantitative research methods were used where data was collected, coded and analyzed with other process parameters, this was achieved after conducting various experiments on the steel bar sample and recording the results in a laboratory guide sheet. Safety and health were strongly observed during each session.

3.1.1 Preparation of specimen for conducting the study

Scrap metals of unknown chemical composition are melted in an induction furnance and casted through a continuous process using a continuous casting machine fitted with a rectangular die to produce the billet. During scrap melting, the amount of carbon and maganesese are highly controlled by either addition of metals having high carbon content into the furnance or neutarlizing the molten metal by addition of metals with less carbon and manganese content like cut-off from iron sheets, this is done in three stages during the melting process to ensure uniform amount of carbon in the billets and at each stage the amount of carbon is determined using strohlein apparatus.

The molten metal in the furnance was scouped by the use of a ladle and cooled to room temperature, one gramm was then loaded into the strohlein apparatus and burned with an equal amount of oxygen in the molecular ratio of 1:1:1, implying that the amount of carbondioxide produced is equal to the amount of carbon in the steel as shown in the equation (i).

$$C_{(s)} + O_{2(g)} \rightarrow CO_{2(g)} \ldots\ldots\ldots\ldots \text{(i)}$$

Its important to note that for low carbon steels the maximum allowable amount of carbon is 0.52% and RRM operates within the range of 0.14% to 0.24% of carbon.

3.1.2 Design of Experiment

The billets having the same carbon content of 0.233% were batched B, D and C. Each batch contains fifteen billets which were then used for the production of a 12 mm , 16 mm and 20 mm rebar respectively. Each hot-rolled rebar size was alternately subjected to controlled cooling by altering the cooling parameters in the experiment.

The cooling parameters used in the study are coolant temperature of 25^0 C, 35^0 C and 45^0 C and a coolant flow rate measured using pressure flow meter at 5 Kgf/cm^2, 10 Kgf/cm^2 and 14 Kgf/cm^2, as illustrated in Figure 3.1. The range of temperatures and pressures above were selected because 25^0C is the minimum value on the temperature scale, while 35^0 C is mid-way and 45^0C is the maximum value on the temperature scale. The same reason mentioned for temperature range selection applies to pressure range selection

The coloured data points were not used in the experiment because the rebar size, coolant temperature and coolant pressure at that point is beyond the calibration of the quench box parameters and it is prone to producing outliers in the results, according to management of RRM.

Parameters such as nozzle position, spray distance, nozzle tip diameter were designed, positioned and calibrated to remit the coolant on to the rebar surface at a flow rate which is sufficient for cooling a specific rebar size. The mill speed and the length of the quench box also dictates on the data points for the experiment (that is to say high speed of the mill on a small rebar size causes the rebar to jump off the roughing rollers before reaching the quench box and it may pass through the quench box faster when it is not cooled sufficiently and vice versa)

Therefore only white data points were considered for experimentation. The experiment were repeated three times per data point considered in order to eliminate errors. So a total of fourty-five experiments were conducted as shown in Appendix 5, instead of eighty one experiments which were suppose to be conducted if there were no limitations of the quenching box.

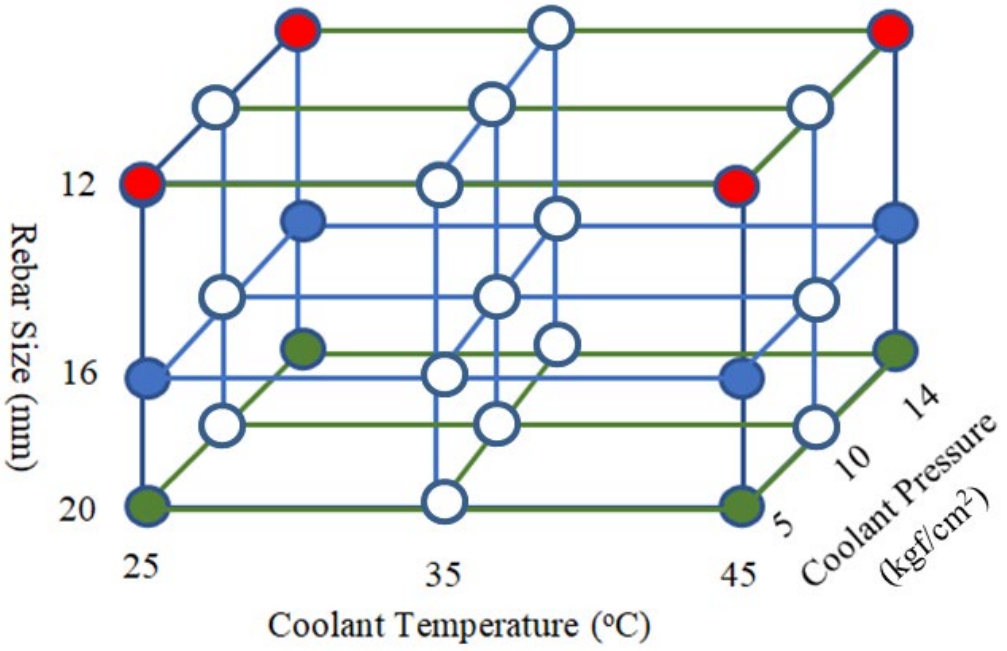

Figure 3.1:.Design of Experiment

3.2 Determination of Chemical Composition of Steel Billets

The chemical analysis was conducted to determine the actual chemical composition of the billets used for the production of the steel bars.

3.2.1 Tools and materials used in chemical Analysis

The tools and materials used in the chemical analysis include; steel billets, cutting machine, grinding machine, polishing machine and mass spectrometer.

3.2.2 Procedure for Chemical Analysis

The chemical analyses were done on steel billets having 0.233% weight of carbon, produced from recycled metal scraps. A batch of fifteen billets having the same amount of carbon were labeled B, which were used to produce 12 mm of steel bars, the second batch having the same amount of carbon were labeled D, which were used to produce 16 mm of steel bars and the third batch having the same amount of carbon were labeled C, which was used to produce 20 mm of steel bars. Each steel billets were cut 25mm across the section and prepared for chemical analysis according to Roofing Rolling Mill Quality Assurance Working Instruction (RRM-QA.WI-07). The prepared specimens were then loaded one at a time into a mass spectrometer and the

elements in the sample were ionized and accelerated, highly charged (more positively charged) elements are lighter in mass and are accelerated most and bends sharply more than heavier ones and are detected first as shown in Figure 3.2.The results were generated automatically using spectromaxsoftwarein a tabular format and recorded.

Polishing machine (a)

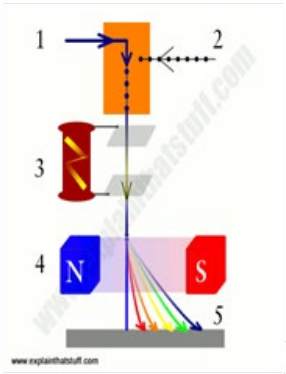

(b)

Figure 3.2: Polishing machine (a) and schematic diagram of principle of a mass spectrometer (b)

3.3 Production of Specimen for Tensile Testing and Microstructure Analysis

The cooling parameters used in the production process during the investigation includes coolant temperature and coolant pressure. The effect of coolant flow rate on tensile strength was determined in this study by altering the coolant pressure flow meter and determining the tensile strength of the rebar. Similarly, the effect of coolant temperature on tensile strength was determined by altering the coolant temperature and determining the tensile strength of the rebar. It involved alternately keeping two parameters constant and then varying the other so as to determine the effect of the variable on strength and microstructure of the rebar. For instance, keeping rebar size and coolant temperature constant and varying flow rate using pressure flow meter.

3.3.1 Equipment and materials used for production of specimen

The equipment and tools used in this experiment were installed at RRM, and available for the production of steel bars. This includes; induction furnace, TMT box, set of rollers of different sizesand steel billets.

3.3.2 Experimental procedure for production of specimens for investigation

Each steel billet in a batch was heated to 1100^0C and alternately keeping two parameters constant and then varying one. The steel billet was hot rolled through different roller sizes to attain the desired rebar size before being cooled in a TMT box as shown in Figure 3-3, the process produced 36 pieces of a 12mm, 16mm & 20mm steel bar, each was 12 meters long and the 18^{th} sample piece was picked from the cooling bed. The 18^{th} sample was chosen for purposes of consistency since it is the median sample number where the parameter levels are consistent.The 18^{th} sample piece was cut into two equal pieces, one for tensile testing and the other for microstructure analysis.The same procedure was repeated for all the steel billets in each batchas shown in Figure 3.3.

Thermo Mechanical Treatment (TMT) Process

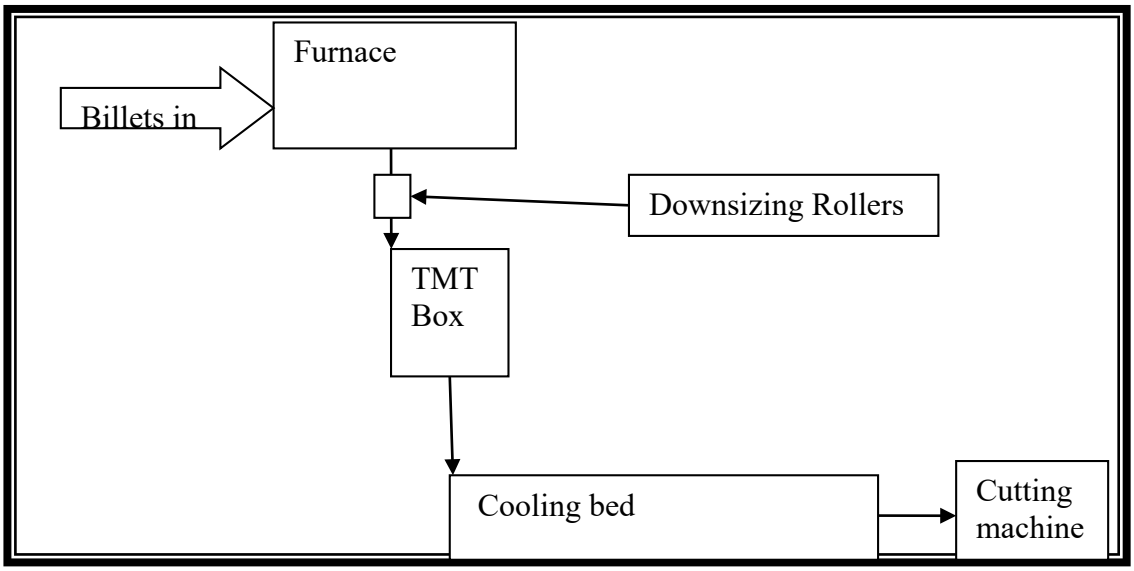

Figure 3.3: Experimental set up of rebar production process

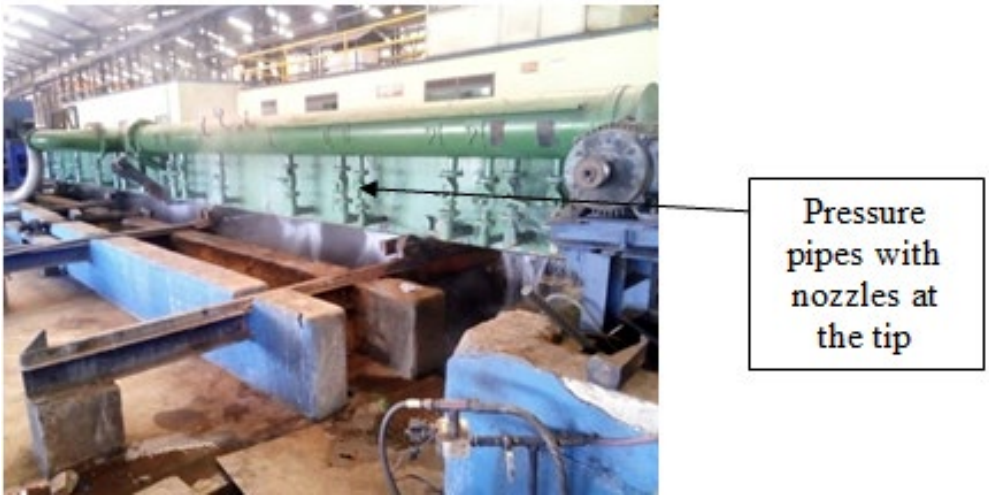

Figure 3.4: TMT box (quenching zone)

3.4 Determination of the effect of cooling parameters on tensile strength of the rebars

This was carried out so as to determine the effect of altering coolant temperature and flow rate, measured using pressure flow meter on the tensile strength of the rebars. This was achieved by carrying out a tensile test on the specimen which was heated and cooled under controlled condition so as to determine the effect of the controlled variable on strength of the rebar.

3.4.1 Equipment and materials for tensile testing

The equipment and materials used for determining the effect of altering coolant temperature and flow rate, measured using pressure flow meter on tensile strength of the rebars includes; Universal Testing Machine connected to a computer, test piece (specimen), calculator, tape measure, center punch, hammer, vernier caliper, bench and angle bar

3.4.2 Experimental procedure for tensile testing

The 18^{th} sample obtained from the cooling bed was cut 500 mm long from the middle portion of the sample. The specimen was weighed and marked in an equal interval of 100 mm using a center punch as shown in Figure 3.5. The weight per meter was obtained and the specimen was loaded onto the UTM. The raw data obtained by direct measurements of the test piece were then fed in to the computer and the loads were applied on to the specimen gradually until fracture. The secondary data like tensile strength, elongation, and yield strength were automatically generated using Universal Testing Machine installed with FIE-100 computer software as shown in Figure 3.6.

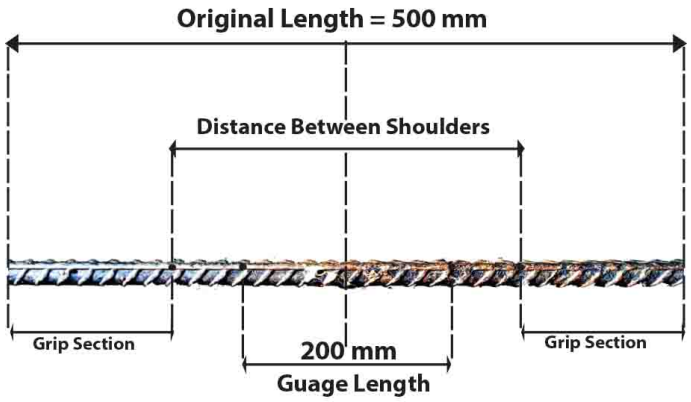

Figure 3.5: Specimen dimensions for tensile testing.

The Gauge lengths were determined using a tape measure and marked to give the reference points within the parallel portion of the specimen. Original lengths were measured using a tape measure while the thicknesses of the specimens along the gauge length were determined using a vernier caliper, the cross-sectional areas and average areas were determined using a calculator and theformula ($A = \pi r^2$).

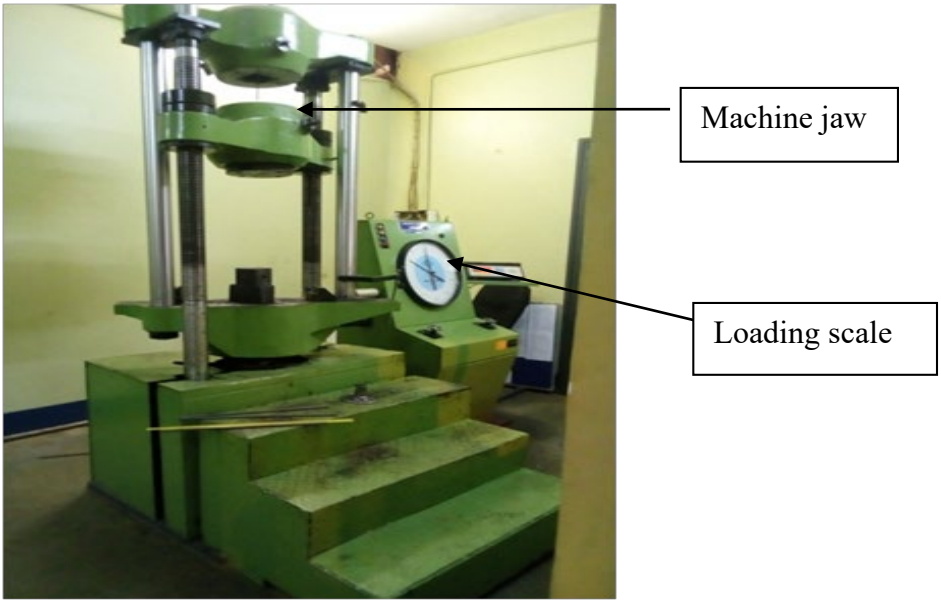

Figure 3.6: Universal Testing Machine, make FIE-100

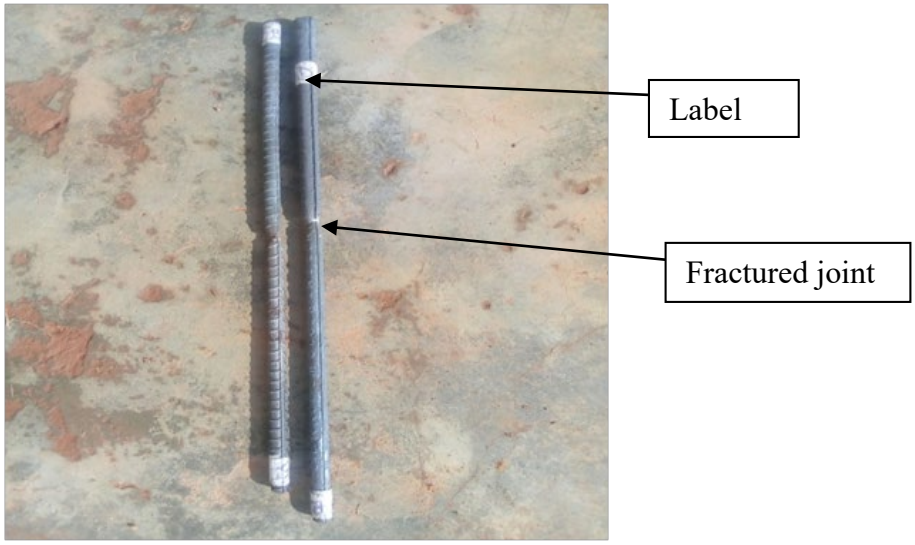

Figure 3.7: Test sample after fracture.

The test results like tensile strength, yield strength, and percentage elongation were automatically generated by Fuel Instrument and Engineers software (FIE-100) and presented in a graphical format of Load-Displacement curves as shown in Appendix7.The same procedure was conducted for all the18thsample obtained from the controlled heat treatment process and tabulated as shown in Appendix 5.

3.5 Determination of the effect of cooling parameters on microstructure

This was done to determine the effect of altering coolant temperature and flow rate, measured using pressure flow meter on the microstructure of the rebars. This was achieved by carrying out microstructure analysis on the specimen which was heated and cooled under a controlled condition so as to determine the effect of the controlled variable on the micro grain structure of the rebar.

3.5.1 Equipment and materials used for microstructure analysis

The equipment and materials used for microstructure analysis include; Cut-off machine, (METASERV Model type C180), Hand grinder model C87, Universal polisher, Sonic cleaner, Hot air dryer, Microscope (Krussoptronic VOPC93) equipped with a camera of 3.0 megapixels

3.5.2 Experimental procedure for microstructure analysis

The experimental procedure was carried out in accordance with Roofing Rolling Mill Quality Assurance Working Instruction (RRM-QA.WI-07) and the micrograph compared with the standards in the metallurgical atlas.The 18^{th} sample obtained from the cooling bed was cut 30 mm long from the middle portion of the sample using a cut-off machine, METASERV Model type C180as shown in Figure 3.8a.The specimen was ground manually using emery papers of grits 220/240, 320, 400 and 600, using hand grinder model C87 as shown in Figure 3.8b.The specimen was then polished using alumina paste on the universal polisher as shown in Figure 3.9 c.This was then cleaned using jet tap water followed by sonic cleaner containing water as shown in Figure 3.9 d.Thereafter the specimen was removed and dried using a hot air dryer as shown in Figure 3.9 e. The dried specimen was etched using 2 % Nital reagent (A mixture of 98% ethanol and 2% concentrated nitric acid) for five seconds as shown in Figure 3.9f. The etched surface was washed again in distilled water and dried. Specimens were examined using Krussoptronic VOPC93 microscope, equipped with a camera of 3.0 megapixels and a micrograph captured at a suitable magnification as shown in Figure 3.8.

Figure 3.8: Observation of microstructure using metallurgical microscope.

Figure 3.9: Preparation of the Specimen for chemical Analysis.

The same procedure was conducted for all the 18th sample obtained from the controlled heat treatment process and the micrographs were compared with those that are found in the American Society of Metals (ASM and AISI) atlas of microstructures of industrial alloys of known chemical compositions and structural conditions. This comparison was done in order to approximate the chemical composition, assess the structural conditions, and obtain grain sizes of the specimen. The results are discussed in chapter four.

Determination of appropriate cooling parameters for the rebars

An appropriate cooling parameters (coolant pressure and coolant temperature) were established after a critical observation made on the mechanical behaviour of rebars subjected to controlled heating and cooling under specific coolant temperatures and coolant pressures. Graphs of UTS, YS and percentage elongation against the cooling parameters were plotted in order to study the relationship in the mechanical behaviour of the specimens.

Specimens which produced strength within the standard limits according to Ugandan Standard and East African Standard(US & EAS 412-2:2013) were considered for the establishment of an appropriate cooling parameters while those specimens which produced strength outside the limits were disregarded.

The cooling parameters together with the UTS of the samples which produced strength within the standard limits were subjected to statistical analysis using established formulaes to calculate the mean, variation of the data and standard deviation as shown in the equation (ii), (iii) and (iv). These were done to understand the deviation from the normal so that an appropriate range of the parameters which are capable of producing strength within the acceptable limits can be established.

$$\text{Mean} = \frac{\sum_{i=1}^{n}(\text{X}_\text{i})}{n} \dots\dots\dots\dots\dots\dots\dots\dots\dots\dots\dots (ii)$$

$$Variance = \sigma^2 = \frac{\sum_{i=1}^{n}(\text{X}_\text{i} - \text{Mean})^2}{n} \dots\dots\dots\dots\dots\dots\dots\dots (iii)$$

$$Standard\ Deviation = \sqrt{Variance} \dots\dots\dots\dots\dots\dots\dots\dots\dots\dots\dots (iv)$$

Having analysed the data statistically, there was need to adjust the experimental design in order to prove and correlate the experimental results and that of the statistical analysis. The experimental design was adjusted as shown in the Table 4.1 and the experimental procedure was repeated using two billets from each batch B, D and C in order to establish an appropriate setting of the cooling parameters.

Table 4.1 Experimental set up for adjusted cooling parameters

S.N	Rebar size [mm]	Coolant temperature [^{0}C]	Coolant pressure [Kgf/cm^2]
1	12	33.5	10
2	12	44.5	14
3	16	35.5	6.8
4	16	44.5	13.2
5	20	26	6.3
6	20	43	13.3

After adjustment of the experimental design to ascertain the effect of adjusting the cooling parameters on strength of the steel bars, the18th sample obtained from adjusted and controlled heat treatment process were then subjected to the same test procedures in Section 3.4.2 were repeated and it is in accordance to RRM-QA.WI-07 for two specimens from each batch B, D and C. The results are tabulated as shown in Appendix 6.

It is important to note that RRM-QA.WI-07 compares exactly the same as ASTM E8/ E8M-13, the slight difference is that RRM-QA.WI-07 have fine instructions customised to the machine model used by RRM to ease the understanding of the operator but does not affect the results obtained

CHAPTER FOUR

RESULTS

The results of the chemical composition, tensile tests, and microstructure investigations are presented in this chapter.

4.1 Chemical Composition of the steel billets

The chemical composition of the steel billets were analyzed and all the alloying elements in the steel billets are included in the Table 4.2**,** while the original format generated by the computer software are attached as shown in Appendix 8**.**

Table 4.2: Chemical composition in weight percentage of steel billets used for rebar production

Alloying Elements [wt.%]									
C	Si	Mn	P	S	Cr	Mo	Ni	Al	Co
0.233	0.313	0.746	0.0350	0.0496	0.0764	0.0099	0.0411	0.0229	0.0018
Cu	Nb	Ti	V	W	Pb	Sn	As	Zr	Bi
0.0917	< 0.0010	0.0014	0.0018	< 0.01	0.0038	0.0151	0.0147	< 0.0015	< 0.004
Ca	Ce	B	Zn	La	Fe	Sb	Te		
>0.0156	< 0.003	0.0048	0.0195	0.003	98.3	< 0.001	< 0.001		

The percentage weight composition of < 0.78% C is hypoeutectic steel and that > 0.78% C is hypereutectic steel, *(Park, 2004).* The experimental results in Table 4-1, shows that the percentage weight composition of carbon for the steel billets were below 0.78% and therefore are low carbon steel (hypoeutectic steel). The approximate chemical composition by weight percentage from metallurgical atlas is shown in Table 4.3

Table 4.3: Approximate chemical composition by weight percentage from metallurgical atlas

Specification	C	Mn	P	S	Type of steel
Billets	0.235	0.740	0.0350	0.0490	Low carbon steel (hypoeutectic steel)

The results revealed that all the billets tested fall within the Uganda Standard and East African standard (US-EAS 412-2013) and the ideal is that the percentage weight composition of carbon must be ≤ 0.25. All the billets used for the production of rebars have 0.233% C, and from literature, it is clear that steel having the same carbon content have similar mechanical behaviour and must posses the same strength *(Valeria et.al, 2015),* and so the expectation is that when the rebar are subjected to the same cooling condition in the quench box then they must posses similarly mechanical behavior due to the fact that the percentage composition of carbon is constant and that carbon controls the mechanical behavior of steel *(Surian et.al, 1991).*

4.2 Effects of size on strength of the rebar

Considering the table showing experimental design and tensile test results in Appendix 5, specimen number one of batch B (12mm rebar), batch D (16mm rebar) and batch C (20mm rebar) were all subjected to the same coolant temperature of 25^0C, and coolant pressure of 10Kgf/cm^2. Specimen number one of batch B (12mm rebar) produced UTS of 686Mpa with 12.01% elongation, that of batch D (16mm rebar) produced UTS of 663.5Mpa with 16.6% elongation while batch C (20mm rebar) produced UTS of 652.35Mpa with 18.01% elongation.

The results showed that strength decreased with increase in rebar size and percentage elongation increased with increase in the rebar size, this is due to the difference in the cooling gradients and transformation rates. A smaller rebar size has a sharp cooling gradient and high transformation rate therefore making it to cool faster than a bigger size of rebar.

4.3Tensile Strength of Rebars as aresult of controlled cooling parameters

The tensile test was carried out to address specific objective two and the graphs which were generated by the FIE-100 computer software installed on the UTM were obtained and shown in Appendix 7 while summery of the results generated by FIE-100 software are tabulated as shown in Appendix 5. Graphs of UTS & YS versus specimen number were plotted to analyze the effect of varying cooling parameter on strength. The graphical presentation of tensile test results for batch B is as shown in Figure 4- 2 and the levels of the cooling parameters are shown in Appendix 2.

4.3.1 Analysis of batch B (12mm rebar)

The results of UTS and YS were plotted graphically and analyzed using a bar graph as shown in Figure 4-2

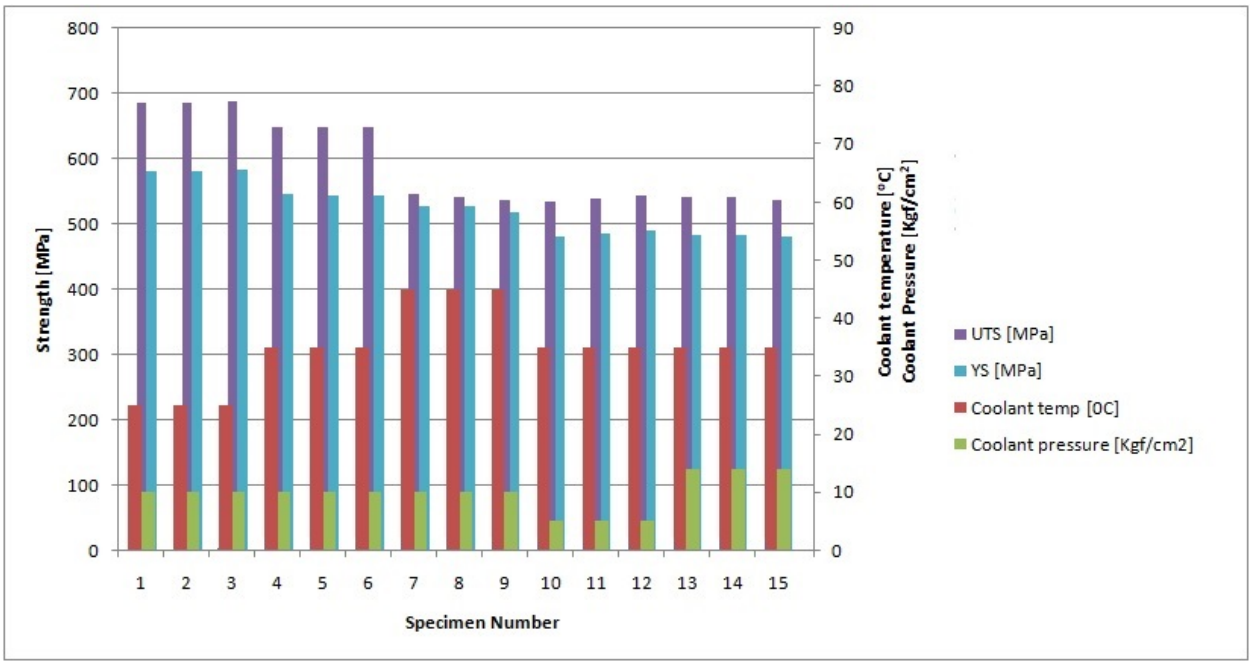

Figure 4.2:UTS and YS of a 12 mm Rebar Versus Specimen Number**.**

Also, a graph of percentage elongation versus specimen number was plotted to analyze the ductility and brittleness of batch B, as shown in Figure 4-3.

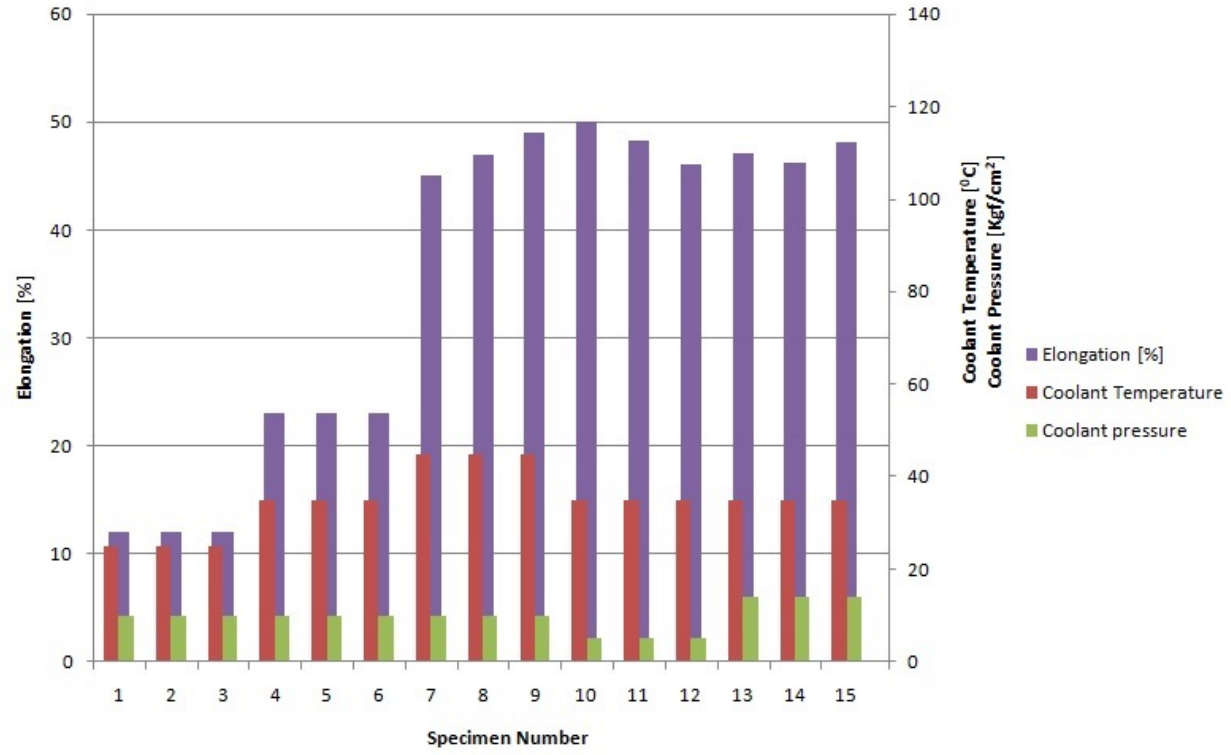

Figure 4.3: Percentage Elongation of a 12 mm Rebar Versus Specimen Number

When a 12 mm hot rebar was subjected to a coolant temperature of 25^0C, at a coolant pressure of 10 Kgf/cm^2, it produced a brittle rebar with percentage elongation of only 12% and a high UTS of 685 MPa, when the coolant temperatures were increased to 35^0C and 45^0C at a constant coolant pressure of 10 Kgf/cm^2, the percentage elongation increased to 23% and 47% and the UTS reduced to 648 Mpa and 542 Mpa respectively, when the coolant temperature was fixed at 35^0C and varied the coolant pressure from 5 Kgf/cm^2 to 14 Kgf/cm^2, the percentage elongation decreased from 48.2% to 46.2% and the UTS increased from 538 Mpa to 540 Mpa respectively. This is due to the fact that at low temperature of the coolant, rapid cooling takes place across the section of the rebar due to the coldness of the coolant, resulting to the formation of martensite which is a hard & brittle material and as the coolant temperature increases, ductility also increases. This is seen in specimen number 5 & 8, but keeping the coolant temperature constant

and increasing the coolant pressure, increases the flow rate, hence reducing ductility as seen in experiment 11 &14.

4.3.2 Analysis of batch D (16 mm rebar)

Graphs of UTS & YS versus specimen number were plotted as shown in Figure 4-4and the cooling parameters are shown in Appendix 3.

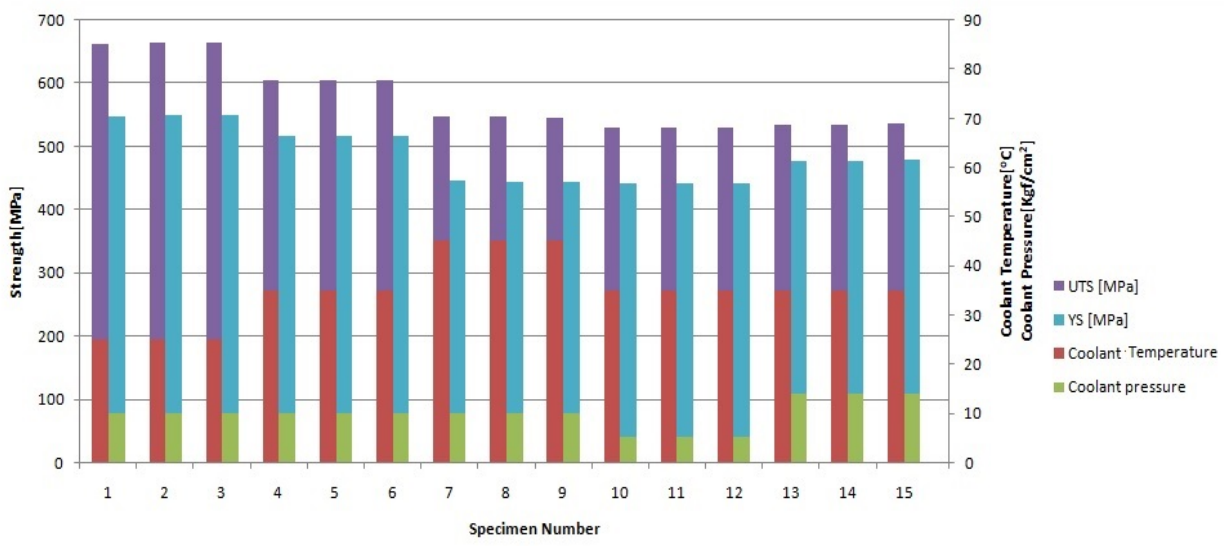

Figure 4.4:UTS and YS of a 16mm Rebar Versus Specimen Number.

Furthermore, a graph of percentage elongation versus specimen number was plotted to analyze the ductility and brittleness of batch D (16 mm rebar) as shown in Figure 4-5.

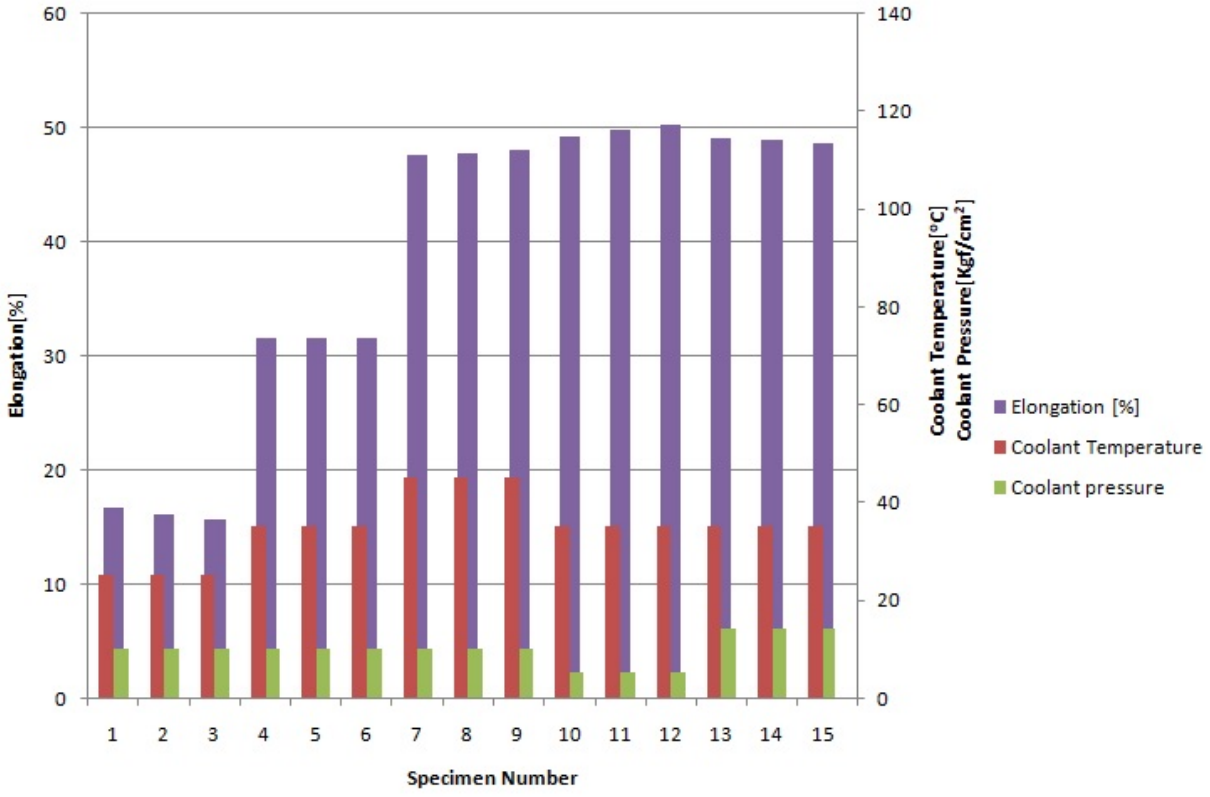

Figure 4.5: Percentage Elongation of a 16 mm Rebar Versus Speciment Number**.**

When a 16 mm hot rebar was subjected to a coolant temperature of 25^0C, at a coolant pressure of 10 Kgf/cm^2, it produced a brittle rebar with percentage elongation of 16.1% and UTS of 664 Mpa, this result produced a less brittle material compared to result in Figure 4-3, this was so, largely because of the differences in the rebar sizes, a smaller rebar may not permit tempering compared to a rebar of bigger size, this has been discussed in Figure 5-1.When the coolant temperature was increased from 35^0C to 45^0C at a constant coolant pressure of 10 Kgf/cm^2, the percentage elongation increased from 31.6% to 47.8% and reduced the UTS from 604 Mpa to 547 Mpa respectively. This was seen in specimen number 5 & 8, but when the coolant temperature was kept constant at 35^0C and the coolant pressure increased from 5 Kgf/cm^2 to 14 Kgf/cm^2, the flow rate increased owing to increased cooling rate of the hot material, the result was reducedductility from 49.8% to 48.9% and increased UTS from 530 Mpa to 535 Mpa as seen in specimen number 11 &14.

4.3.3 Analysis of batch C (20 mm rebar)

Graphs of UTS & YS versus specimen number were plotted to analyze the effect of varying cooling parameter on strength of C (20 mm rebar) as shown in Figure 4-6 and the cooling parameters are shown in Appendix 4.

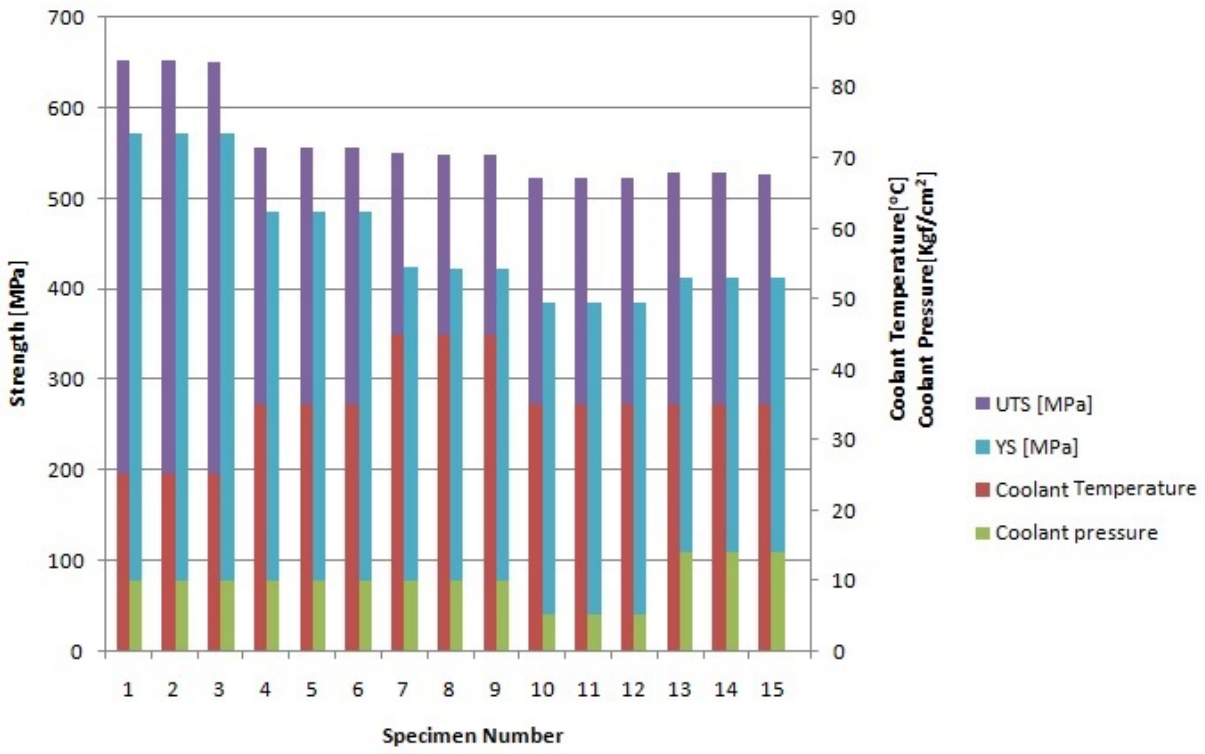

Figure 4.6:UTS and YS of a 20 mm Rebar Versus Specimen Number.

To analyze the ductility and brittleness of C (20mm rebar), a graph of percentage elongation versus specimen number was plotted as shown in Figure 4-7.

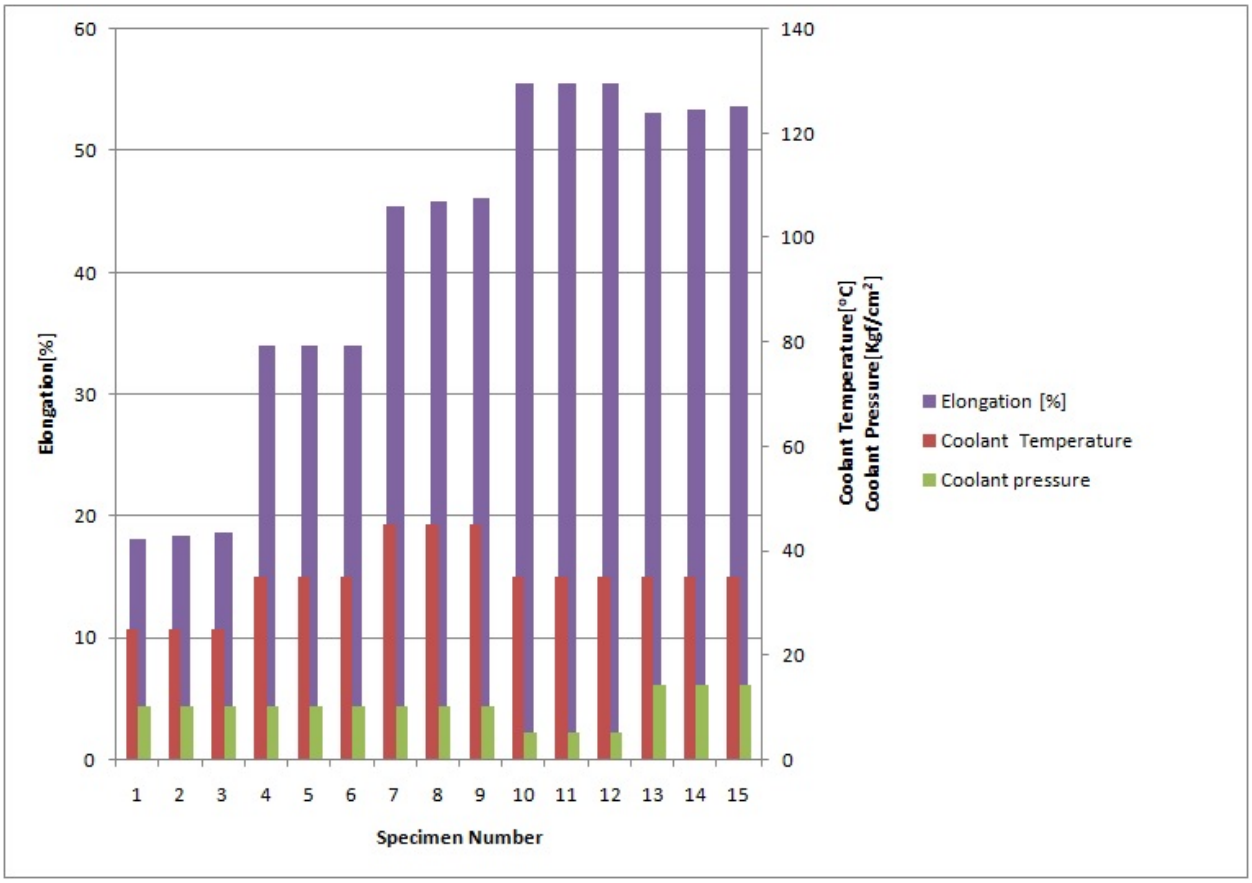

Figure 4.7: Percentage Elongation of a 20 mm Rebar Versus Specimen Number.

When a 20 mm hot rebar was subjected to a coolant temperature of 25^0C, at a coolant pressure of 10 Kgf/cm^2, it produced a brittle rebar with percentage elongation of 18.3% and UTS of 652 Mpa, this result produced a less brittle material compared to result in Figure 4-5, this was due to the differences in the rebar sizes, a smaller rebar may not permit tempering compared to a rebar of bigger size, this has been discussed in Figure 5-1. When the coolant temperature was increased from 35^0C to 45^0C at a constant coolant pressure of 10Kgf/cm^2, the percentage elongation increased from 31.6% to 47.8% and reduced the UTS from 557Mpa to 549MPa respectively. This was seen in specimen number 5 and 8, but when the coolant temperature was kept constant at 35^0C and the coolant pressure increased from 5Kgf/cm^2 to 14Kgf/cm^2, the flow rate increased resulting to increased cooling rate of the hot material, the result was reduced ductility from 49.8% to 48.9% and increased UTS from 522Mpa to 528Mpaas seen in specimen number 11 and 14.

4.4 US-EAS 412-2:2013 Standard

The strength of the specimen was compared with the standard according to Uganda National Bureau of Standards (UNBS) and used as a basis to either reject or accept the quality of the rebar. The standard limits are as shown in Table 4.4

Table 4.4:US-EAS 412-2:2013 Standard tensile testing results.

UTS[Mpa]	YS [Mpa]	UTS:YS	% Elongation
550-650	450-550	1.15-1.19	20-45

4.5 Critical observation made from the experiments conducted

Experiment 2, 7 and 12 conducted on rebar size 12 mm, 16 mm and 20 mm respectively, were subjected to a coolant temperature of 35^0C and a coolant pressure of 10Kgf/cm^2, as shown in Appendix 5. The result revealed UTS of 648 MPa, 604 MPa and 549 MPa respectively, were within the acceptable limits according to US-EAS412-2:2013 standards. But important to note is that 648MPa lies towards the upper limit of the standard range, 604 MPa lies mid-way of the range and 549MPa lies towards the lower limit of the standard limit, respectively.

Determination of appropriate settings of the cooling parameters

The cooling parameters together with the UTS of the samples which produced strength within the standard limits were subjected to statistical analysis using established formulaes to calculate the mean, variation of the data and standard deviation as shown in the equation (ii), (iii) and (iv). This was to understand the variation of the data from the normal and the following results were obtained and ploted on a normal distribution curve to demonstrate the deviation from the mean.

For a 12 mm rebar, the mean of the Coolant temperature was 39^0C with a standard deviation of 5.5^0C. The mean of the Coolant pressure was 12Kgf/cm^2 with a standard deviation of 2 Kgf/cm^2 and the mean of UTS was 602 MPa with a standard deviation of 46 MPa.

For a 16 mm rebar, the mean of the Coolant temperature was 40^0C with a standard deviation of 4.5^0C. The mean of the Coolant pressure was 10 Kgf/cm^2 with a standard deviation of 3.2 Kgf/cm^2 and the mean of UTS was 598.5 MPa with a standard deviation of 44.5 MPa.

For a 20 mm rebar, the mean of the Coolant temperature was 35^0C with a standard deviation of 8^0C. The mean of the Coolant pressure was 9.8 Kgf/cm^2 with a standard deviation of 3.5 Kgf/cm^2 and the mean of UTS was 601.5 MPa with a standard deviation of 43.5 MPa.

Statistical analysis for a 12 mm rebar, batch B

12 mm Rebar

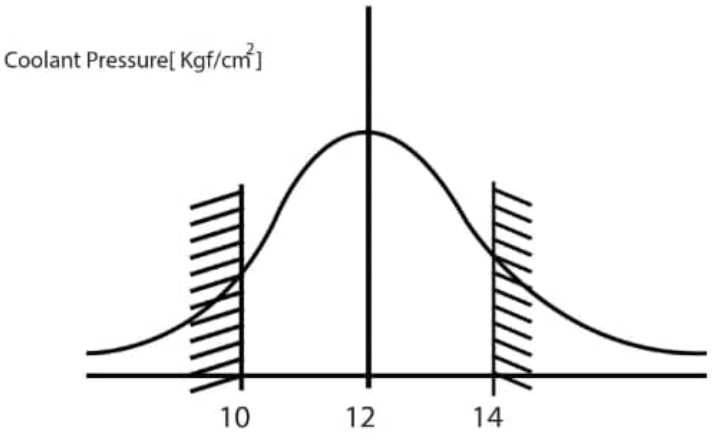

$\overline{x} = 12$

$\sigma = 2$

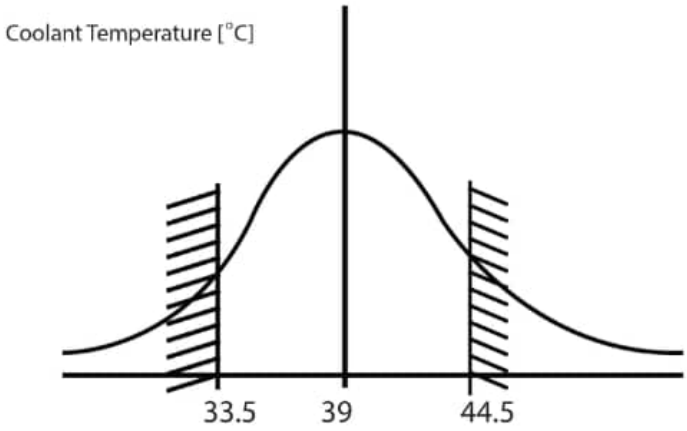

$\overline{x} = 39$

$\sigma = 5.5$

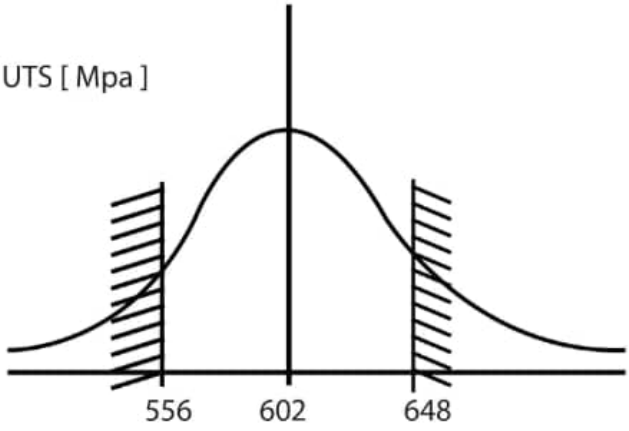

$\overline{x} = 602$

$\sigma = 46$

Statistical analysis for a 16 mm rebar, batch D

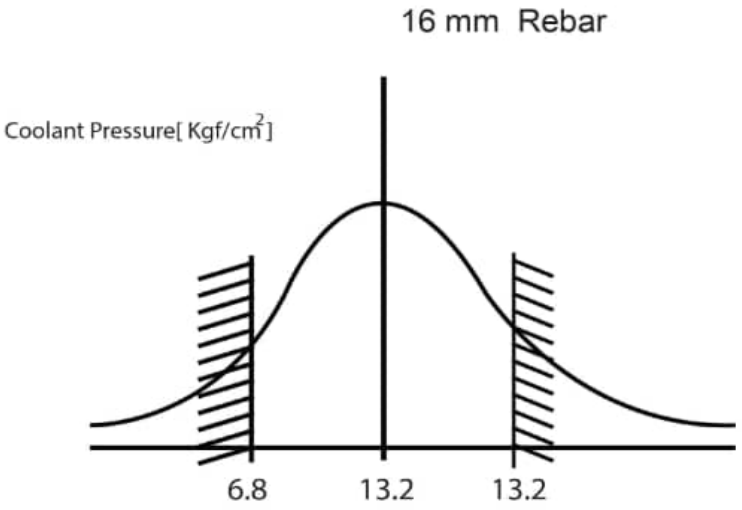

$\overline{x} = 10$

$\sigma = 3.2$

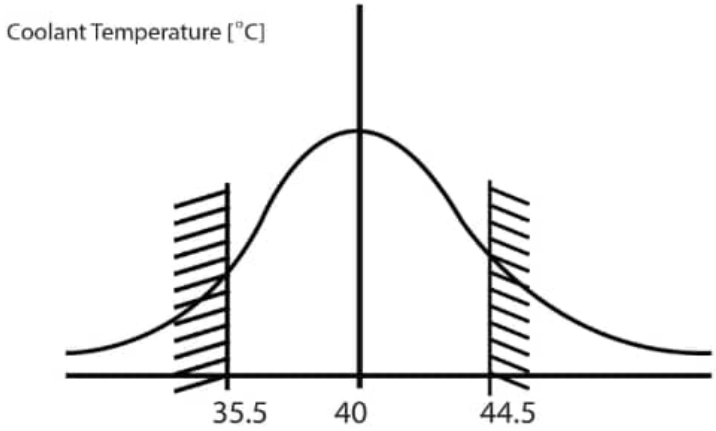

$\overline{x} = 40$

$\sigma = 4.5$

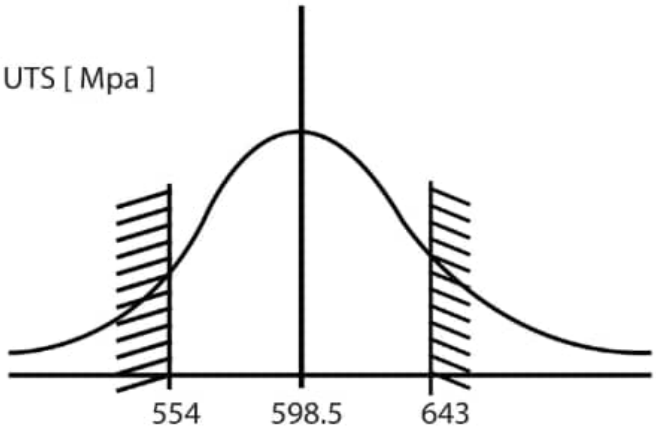

$\overline{x} = 598.5$

$\sigma = 44.5$

Statistical analysis for a 20 mm rebar, batch C

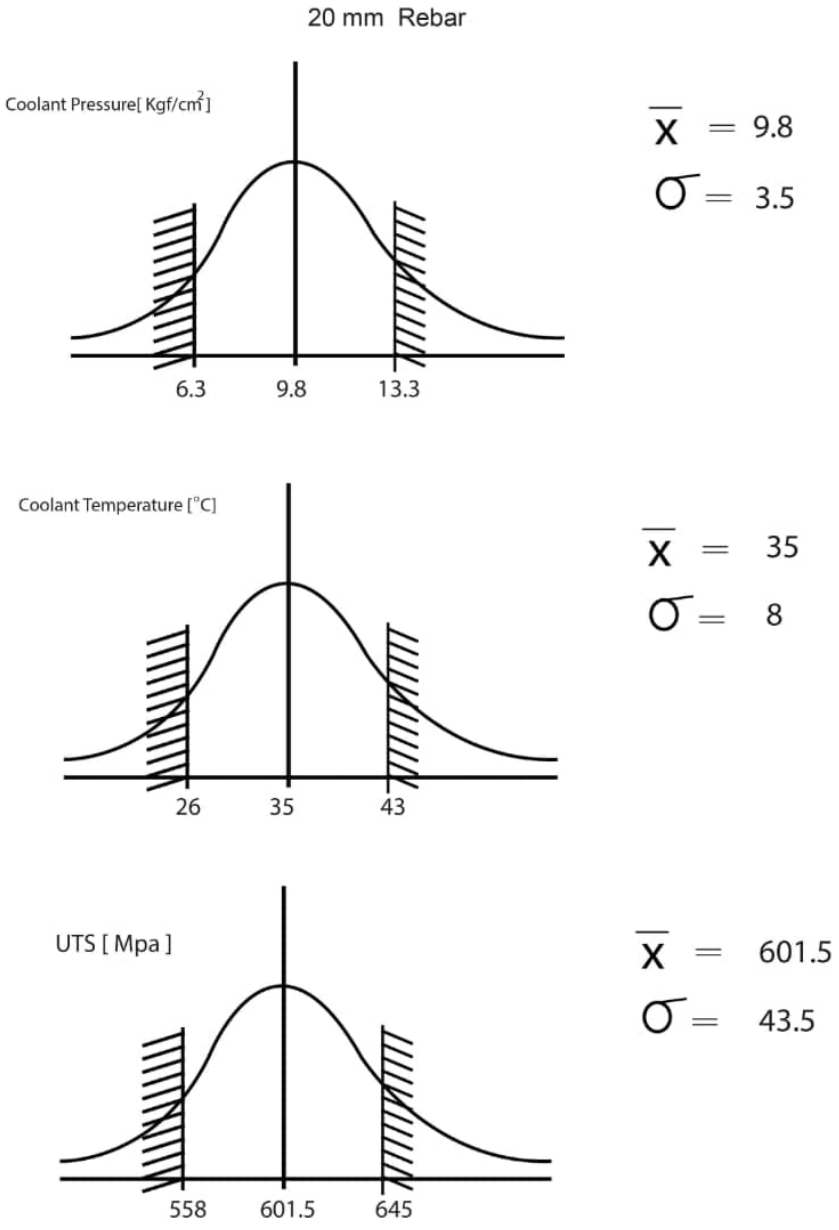

4.6 Experimentation of the new Coolant Temperature and Coolant Pressure settings

The adjustments of cooling parameters were done as per the statistical analysis results and the experiments conducted to prove if this results will yield strengths within the limits of the US & EAS 412-2:2013 Standard. The results of the experiment were obtained and analyzed graphically as shown in Figure 4-8 and Figure 4-9.

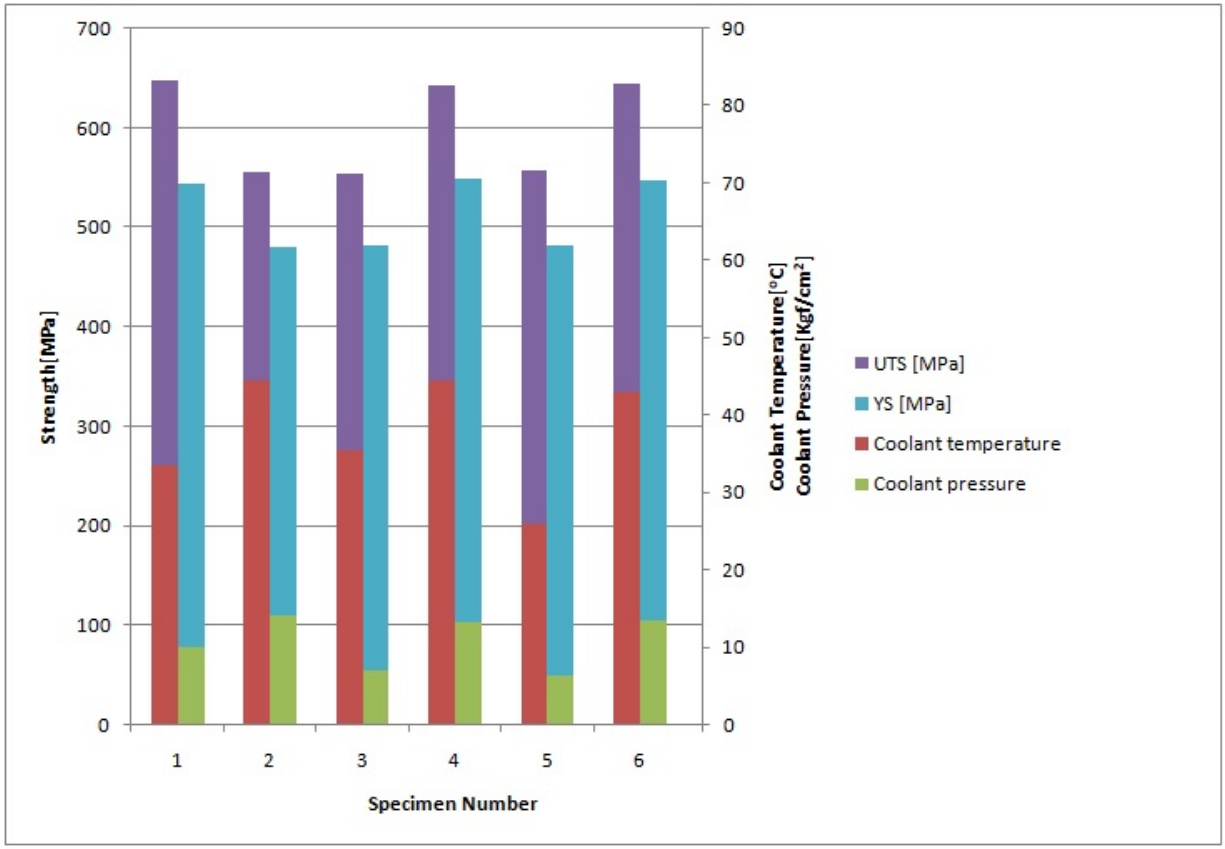

Figure 4.8: UTS &YS after adjustments of cooling parameter

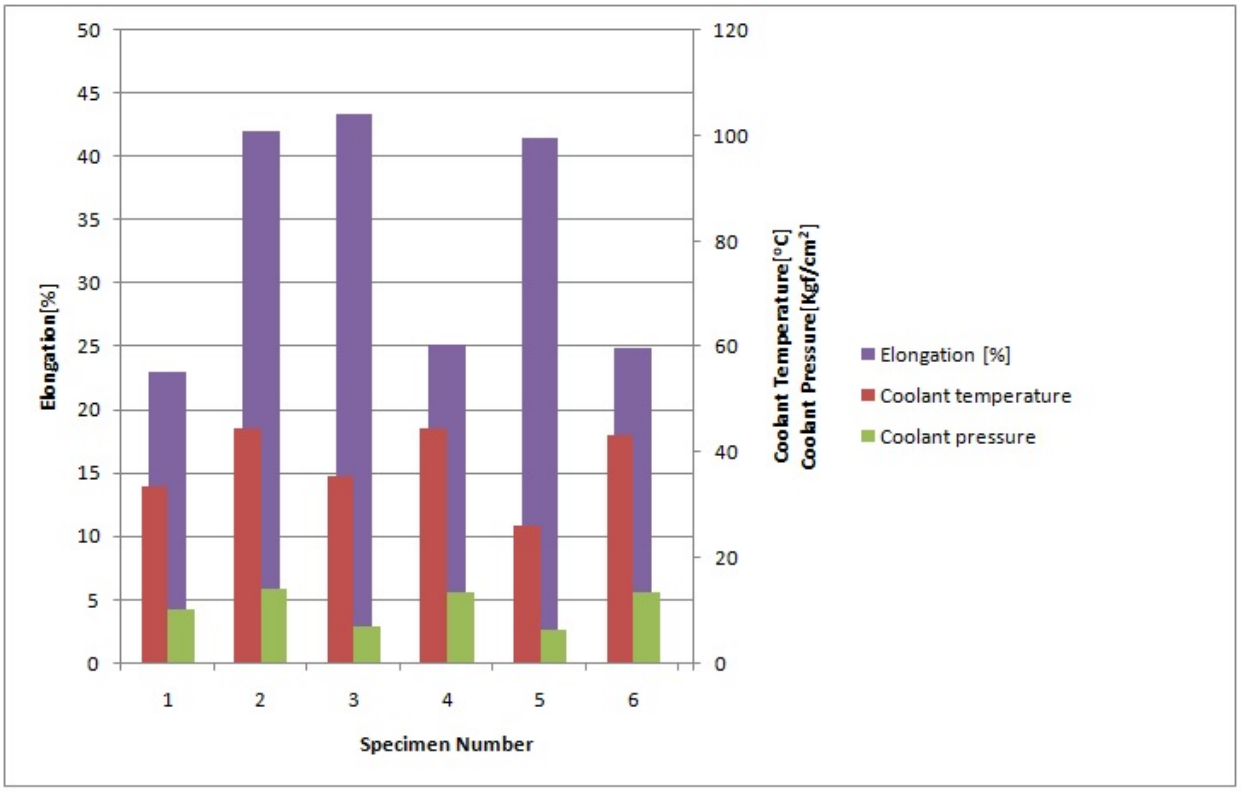

Figure 4.9: Percentage elongation after cooling parameter adjustment.

Specimen 1 (12 mm rebar), subjected to a coolant temperature of 33.5^0C, at a coolant pressure of 10 Kgf/cm^2, produced UTS of 648.04 Mpa and elongation of 23%, Specimen 2 (12 mm rebar), subjected to a coolant temperature of 44.5^0C, at a coolant pressure of 14 Kgf/cm^2, produced UTS of 556.035 Mpa and elongation of 42%. Specimen 3 (16mm rebar), subjected to a coolant temperature of 35.5^0C, at a coolant pressure of 6.8 Kgf/cm^2, produced UTS of 553.85 MPa and elongation of 43.4%, Specimen 4 (16 mm rebar), subjected to a coolant temperature of 44.5^0C, at a coolant pressure of 13.2 Kgf/cm^2, produced UTS of 643.09 MPa and elongation of 25.1%. Specimen 5 (20 mm rebar), subjected to a coolant temperature of 26^0C, at a coolant pressure of 6.3 Kgf/cm^2, produced UTS of 557.79 MPa and elongation of 41.5%, Specimen 6 (20 mm rebar), subjected to a coolant temperature of 43^0C, at a coolant pressure of 13.3 Kgf/cm^2, produced UTS of 645.063 MPa and elongation of 24.8%. All these results lie within the US &EAS 412-2:2013, when compared with results in Appendix 6

4.7 Microstructure of the Specimen Subjected to the Same Heat Treatment Condition

The micrograph of different sizes of rebars (i.e. 12mm, 16mm and 20mm) subjected to a coolant pressure of 10 Kgf/cm^2 and coolant temperature of 35^{0}C, (i.e. the same heat treatment condition) were obtained and displayed as in the Figure 4-10

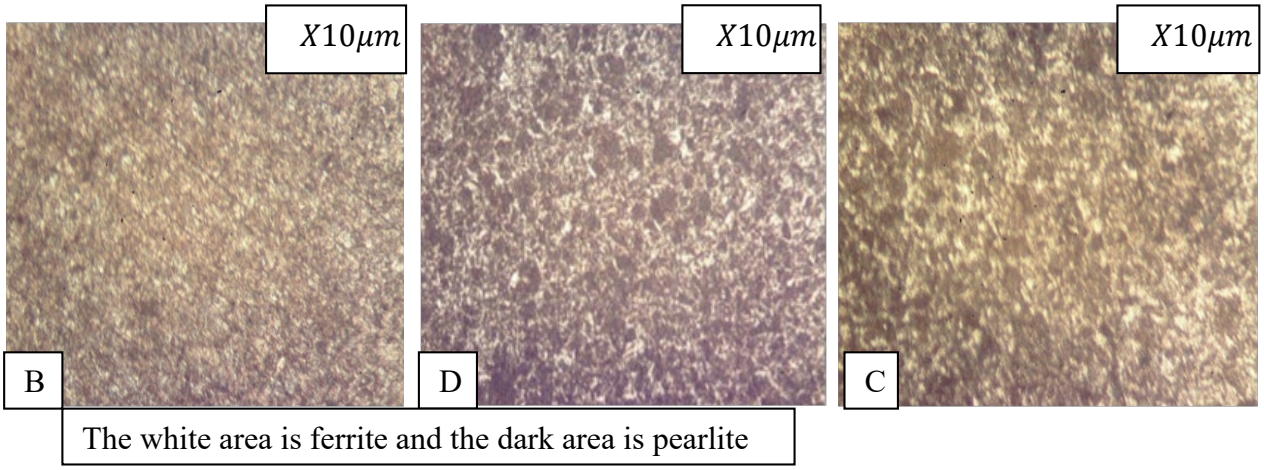

Figure 4.10: Micrograph of 12,16, & 20 mm rebar subjected to the same heat treatment

Micrograph B (12mm rebar) has numerous small and dark grain structure (pearlite) distributed on the outer surface of the micrograph and few small white grain structure (ferrite) sparsely distributed at the center of the micrograph with no clear lines of the grain boundaries. Micrograph D (16mm rebar) has a bigger grain structure compared to B and a matrix mix of both the pearlite and ferrite evenly distributed across the entire surface with clear grain boundaries. Micrograph C (20mm rebar) has bigger grains compared to D, with clear grain boundaries and more distribution of ferrite than pearlite on the entire surface. From *Surian et.al, (1991)* it can be deduced that B has more strength than D and D has more strength than C, however ductility decreased from C to D.

4.8 Microstructure of the specimen after adjusting cooling parameters

The micrographs obtained after adjustments of cooling parameters were nearly appearing the same and only two micrographs were discussed in the analysis as shown in Figure 4-11

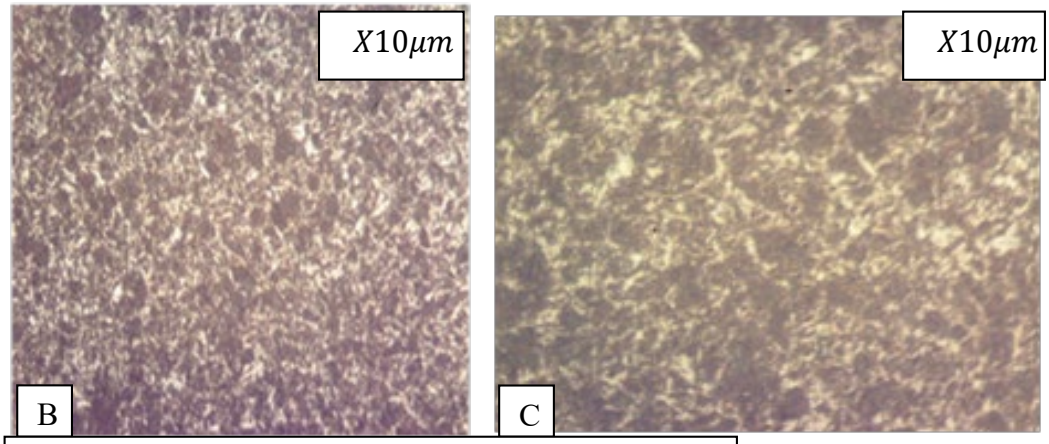

Figure 4.11: Micrograph of 12 & 20 mm rebar after adjusted cooling condition

The microstructure in Figure 4-11 (B) has fine grain structure mixed uniformly with both pearlite and ferrite which is evenly distributed in the entire surface of the micrograph. Figure 4-11 (C), has visible grain boundaries, coarse grain structure mixed uniformly with both pearlite and ferrite which is evenly distributed in the entire surface of the micrograph.

CHAPTER FIVE

DISCUSSION OF RESULTS

The results of the chemical composition, tensile tests, and microstructure investigations are discussed in this chapter.

5.1 Chemical Composition of Rebars

The Billets used for the production of the rebars contained more than twenty alloying elements as shown in Table 4-1, all these elements have varied significant effect on the mechanical behaviour of steel. Carbon has the effect of increasing strength and so the more carbon the more strength of the material, *(Callister et.al, 2008).* Increasing the amount of nitrogen increases hardness and yield strength and decreases the tensile elongation, *(Witmer D.A and Willison R.M 1970),* On the other hand addition of **a**luminium leads to a decline of tensile strength, the yield strength and elongation (*Haifeng XU et.al,2015).*

Silicon has the effect of deoxidizes steel by dissolving in iron and removing bubbles of oxygen from the molten steel *(Drumond et.al, 2012).*Manganese just like silicon, increases the rate of carbon penetration during carburizing and acts as a mild deoxidizing agent and responsible for taking the sulphur and oxygen out of the melt into the slag, however when too high carbon and too high manganese accompany each other, embrittlement sets in *(Leslie W.C. 1987).* Manganese also combines with sulphur to form Manganese Sulphide (MnS), which is beneficial to machining however its ratio greatly affects weldability of steel.

Copper has a small impact on hardenability and it increases the corrosion resistance of steel due to the formation of a very thin oxide film on the steel surface, its amount in steel is not less than 0.20 percent (*Yamashita .M et al, 1998),* (*Schwabe .K 1971).*

The effect of size on tensile strength of the rebar

Irrespective of the cooling parameters (a type of coolant, flow rate, coolant temperature) as long as the cooling parameters are applied uniformly across the rebar, rebar having a small diameter (cross-sectional area) cools faster than rebar having a bigger diameter (cross-sectional area). This is is due to the difference in the cooling gradient and transformation rates as discussed further with the aid of a Time Temperature Transformation (TTT) curve in Figure 4-2.

The cooling trend of hot-rolled rebar (TTT curve)

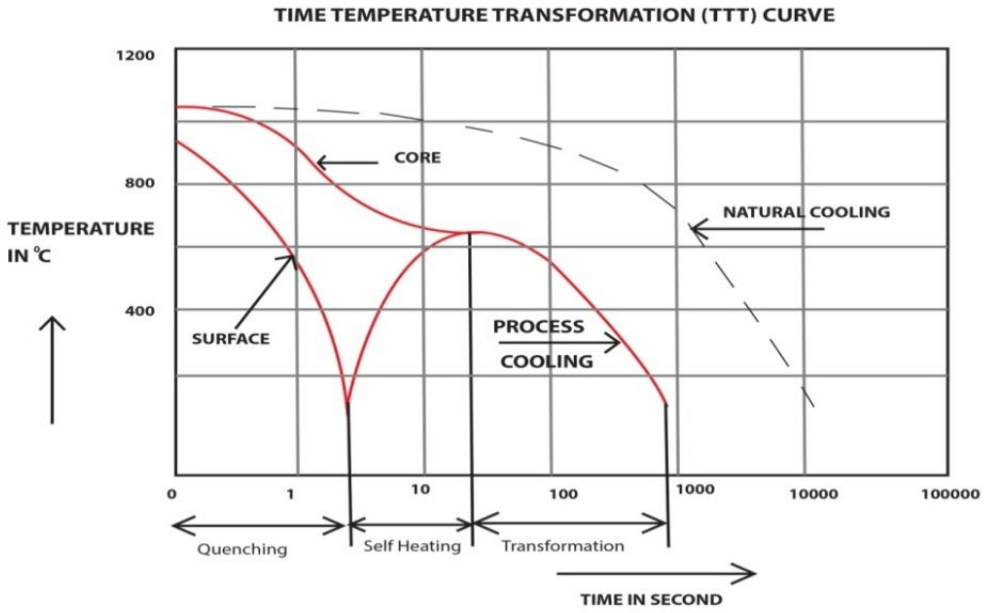

Figure 5.1: TTT curve for spray quenched rebar

When the quenchant (coolant) strikes the surface of the rebar, during pressurized spray quenching, cooling takes place faster on the surface, while the inner core remains hot, after a while the outer surface is reheated by heat from the inner core of the rebar during the process of tempering (cooling by natural air) to ambient temperature on the cooling bed, as shown by the solid lines in Figure 5-1, however the cooling curve follows the dotted lines, when the hot rebar is quenched in a bath to ambient temperature. Therefore the mechanical properties such as ductility, hardenability, tensile strength, yield strength, and percentage elongation will depend on

the pre-set pressure of coolant spray and the quenchant temperature in contact with the hot rebar during the heat treatment process.

When different rebar sizes are accorded the same cooling treatment, a smaller rebar size cools faster and becomes less ductile due to the fact that the rebar core is near the surface, so when the pressurized spray of coolant strikes the rebar surface,both the rebar core and the rebar surface cools faster at the same cooling rate, leaving no time for tempering (self-reheating by the hot rebar core and cooling naturally to ambient temperature by air). A bigger rebar size has the core far away from the surface and given the processing speed (speed of the rolling mill), pressurized spray of coolant strikes the rebar surface and cools the surface faster leaving the rebar core still hot, this permits tempering, hence facilitating the formation of a matrix mix of pearlite and ferrite in the microstructure.

Furthermore, if the cooling rate is too rapid on the rebar surface, nucleation and growth mechanisms occurs at a critical cooling rate *(Park 2004)*, the end result is that carbon is trapped and forced into the crystalline lattice so that instead of forming ferrite structures, the austenite lattice shears and forms a body-centered tetragonal structure called martensite.The martensitic transformation occurs without diffusion of the carbon and therefore occurs very rapidly. In addition, once the austenitic structure is undercooled to the point at which the carbon cannot diffuse and additional ferrite cannot form, the only remaining transformation that can occur upon further cooling is to martensite.

5.3 Effect of Coolant Temperature and coolant pressure on Tensile Strength of Rebars

Low water pressure of 5 Kgf/cm^{2}results to low flow rate, so when the rebar enters the quenching zone, water flows slowly over the rebar irrespective of the mill speed, here very little structural transformation takes place due to the high speed of the rolling mill, resulting into the formation of austenite plus cementite, above 723℃, and later tempered to ferrite. This leads to the dominance of ferrite (white and soft) in the microstructure hence less strength of the rebar as seen in the results of Experiment 4, 9 and 14**.** But high-pressure results into high flow rate hence rapid cooling, leading to the formation of martensite which is hard and brittle, during self-reheating by the core, very little heat is dissipated to the surface due to over-cooling, the end

result is the formation of a matrix mix of martensite and pearlite, with martensite dominating the microstructure.

At low coolant temperature (25^0C), rapid cooling takes place due to the coldness of the water falling on the surface of the hot rebar leading to the formation of a matrix mixture of martensite and pearlite. But at high coolant temperature (45^0C), the coolant is ineffective due to the hotness, this result into slow cooling of the rebar. The dominance of ferrite explains the ductility as seen in experiment 5, 10 and 20. Therefore a balanced setting of coolant temperature and coolant pressure would facilitate the formation of a mixed matrix of martensite and pearlite with some traces of ferrite, due to self-reheating by the heat from the core of the rebar.

5.4 Effect of Coolant Temperature and coolant pressure on Microstructure of Rebars

Low water pressure of 5Kgf/cm^2 results to low flow rate, so when the rebar enters the quenching zone, water flows slowly over the rebar irrespective of the mill speed, here very little structural transformation takes place due to the high speed of the rolling mill, resulting into the formation of austenite plus cementite, above 723℃, and later tempered to ferrite. This leads to the dominance of ferrite (white and soft) in the microstructure hence high ductility of the rebar as seen in experiment **4, 9 and 14.**

High coolant pressure of 14Kgf/cm^2, results to increased flow rate owing to rapid cooling of the hot material, this facilitates the formation of more pearlite than the ferrite in the microstructure, resulting to reduced ductility from 49.8% to 48.9% and increased UTS from 530Mpa to 535Mpa as seen in specimen number 11 and 14.

5.4.1 Effect of rebar size on strength and microstructure of the rebar

During the transformation of the rebar, the structure changed rapidly to martensiteand pearlite due to rapid cooling of both the core and surface of the rebar resulting to the formation of numerous fine grain structure of pearlite mixed with ferrite, this was evident in Figure 4-10 (B) and this explains the reason for UTS of 648 Mpa and a percentage elongation of 23%, which is tending to a brittle status but within the US & EAS 412-2:2013.

When a bigger rebar of size16mm was subjected to the same heat treatment condition, rapid cooling took place on the surface of the rebar and later tempered by the heat of the hot core, leading to the formation of a uniform matrix mix of pearlite and ferrite in the microstructureas seen in Figure 4-10 (D),resulting to UTS of 604 Mpa and percentage elongation of 31.6%, this showed increased ductility compared to a 12 mm rebar. For a 20 mm rebar, Figure 4-10 (C),treated similarly showed a coarse uniform distribution of a mixture of pearlite and ferrite in the microstructure, which was responsible for UTS of 557Mpa and percentage elongation of 34%, this showed increased ductility compared to 16mm and 12mm rebar respectively.

5.5 Metallurgical Comparison with the standards.

The metallurgical atlas considers the relevance of four key important elements,namely carbon, Manganese, Phosphorous and Sulphur whose individual effect/ combined effects have a significant impact on the microstructural characteristics of steel. Table 4- 1, shows how the micrograph has been compared with the standards in the metallurgical atlas

Table 5.1: Comparison of the experimental micrograph with standard metallurgical atlas.

Figure	Expt. Sample number (table 3-4)	Experimental microstructure description	Atlas Standard microstructure description	Steel type recommendation
4-10	5 (B)	Many small grains of pearlite & few ferrites	martensite matrix, mixed with pearlite fine recrystallized ferrite grains	Low carbon steel (hypoeutectic steel) Good yield
4-11	4 (B)	More pearlite & ferrite in the core than on the surface	A mixture of ferrite and pearlite on the outer surface	Low carbon steel (hypoeutectic steel) Bad yield
4-10	5 (B)	Fairly coarse pearlite & ferrite	Ferrite (white area), Pearlite (dark grey), Bainite on the outer surface	Low carbon steel (hypoeutectic steel) Good yield

4-11	9 (D)	Coarse grain of pearlite and more ferrite	Fibrous structure(circular ferrite), Large dark pearlite, covering the entire surface	Low carbon steel (hypoeutectic steel) Bad yield
4-10	5 (C)	A fairly coarse mixture of pearlite & ferrite	pearlite mixed with fully recrystallized ferrite grains 20	Low carbon steel (hypoeutectic steel) Good yield
4-11	14 (C)	Sparsely distributed coarse grains of pearlite & ferrite	Black constituents of, Matrix of ferrite	Low carbon steel (hypoeutectic steel) Bad yield

5.6 Effects of appropriate cooling parameters on microdtuctre of rebars

After adjustments on the cooling parameters was done, micrograph in Figure 4-11, was arrived at and Figure 4-11 (B), showed fine grain structure of pearlite and ferrite uniformly distributed on the entire rebar surface, resulting to a less ductile material with percentage elongation of 23%. Micrograph in Figure 4-11 (C), showed coarse grain structure of pearlite and ferrite uniformly distributed on the entire rebar surface, resulting to a more ductile material with percentage elongation of 41.5%. Generally, ductility increased with an increase in grain size especially when different sizes of rebars are subjected to the same heat treatment condition.This results is consistent with the findings of other researchers in the literature. According to *Shizhong, (2006).*Particle size increases with higher tempering temperature and/or a longer time, hence making the material softer and more ductile.

CHAPTER SIX

CONCLUSIONS AND RECOMMENDATIONS

This research has been completed successfully with all the objectives and research questions met and so this chapter covers conclusions and recommendations for process improvement and further research in this area.

6.1 Conclusions

This research focused on the effect of heat treatment processes on the strength of different sizes (i.e. 12mm, 16mm, and 20mm.) of hot-rolled rebars. Controlled cooling was done on the rebar by altering the coolant pressure and coolant temperature one at a time during the cooling process, both tensile test and microstructure analysis was done on specimens and arrived at the conclusion below

The implementation of these conclusions will enable RRM to realize a significant reduction on the number of rejects of the rebars and reduce on the financial loss of the company.

The specific objective one has been achieved and the results presented in Table 4.1 and also summerised in conclusion one.

Conclusion one: The summery of Chemical composition of steel billets used in the experiment

Alloying Elements [wt.%]									
C	Si	Mn	P	S	Cr	Mo	Ni	Al	Co
0.233	0.313	0.746	0.0350	0.0496	0.0764	0.0099	0.0411	0.0229	0.0018
Cu	Nb	Ti	V	W	Pb	Sn	As	Zr	Bi
0.0917	< 0.0010	0.0014	0.0018	< 0.01	0.0038	0.0151	0.0147	< 0.0015	< 0.004
Ca	Ce	B	Zn	La	Fe	Sb	Te		

>0.0156	< 0.003	0.0048	0.0195	0.003	98.3	< 0.001	< 0.001

Table 6.1: Summary of the appropriate cooling parameter range after experimentation

Rebar size [mm]	Coolant temperature rang [^{0}C]	Coolant pressure range [Kgf/cm^2]
12	33.5 to 44.5	10 to 14
16	35.5 to 44.5	6.8 to 13.2
20	26 to 43	6.3 to 13.3

6.2 Recommendations

6.2.1 Recommendations for the heat treatment process

In order to harness the benefits like reduced production losses and rejects produced during the production run, there is need to focus more on; improvement of the cooling tower efficiency and effectiveness so that even temperatures below room temperatures can be achieved during cooling, installation of pyrometers or an Infrared Thermometer (IR) to monitor the temperature of the rebar along the production line. In the absence of online temperature tracking, improvement of the TMT box efficiency through routine service of the spray nozzles, installation of flow meter to measure directly the flow rate rather than using pressure flow meter.

6.2.2 Recommendation for further research.

Further research could focus on the determination of the effect of tempering time on strength of the rebar during natural cooling on the cooling bed since most technicians at the physical laboratory of RRM are observed to use forced cooling using cold blowing air from the fan which greatly affects tempering time, microstructure and strength of the rebar.

REFERENCES

Adnan, Narayanasamy R, Anandakrishnan V, 2010, “effect of the carbon on the stress-strain behavior in the low carbon steels”. Australia, p. 483

Alberg. H. 2003 MaterialModelling for Simulation of Heat Treatment. Unpublished Master of Science Thesis, Lulea University of Technology, Lulea.

Alondaoui Jamal Nevin 2009 "effect partial thermal treatment on the mechanical properties of the solid high-carbon used in preparing the active parts of the pieces of the mold on the cold cutting, " Engineering and Technology magazine, Aalcild 27, No. 5 Industry.

American Iron and Steel Institute (AISI) and Society of Automotive Engineers (SAE) ASME 2002 ASM handbook, volume.

Bohumil .T, Steven.D.andSpanielka.J.S, 2012, Effect of Agitation Work on Heat Transfer during Cooling in Oil Isorapid 277HM. Journal of Mechanical Engineering, 58, 102-106.

CallisterJr .D, Wiley J & Sons, NY, 2008.Fundamentals of Materials Science and Engineering, 3rd Ed.

Chabicovsky .M, Hnizdil .M, Tseng .A. A, Raudensky .M, 2015, Effects of Oxide Layer on Leidenfrost Temperature during Spray Cooling of Steel at High Temperatures, International Journal of Heat and Mass Transfer, 88 236–246, doi:10.1016/j.ijheatmasstransfer. 2015.04.06

Chabicovsky .M, Raudensky .M, 2013 Experimental Investigation of a Heat Transfer Coefficient, Mater.Tehnol., 47 3, 395–398 2

Chen .J.H, Wang .G. Z, and Hu .S.H, 2001. Metall. Mater.Trans. A 32, 5

Chen .R.-H, Chow .L.C and Navedo. J.E, 2002 Effects of spray characteristics on critical heat flux in subcooled water spray cooling, Int. J. Heat Mass Transfer 45 4033–4043.

Collinson .D. C, Hodgson .P. D, and Davies .C.H. J, 1997 in Thermec'97, Wollongong, "effect of the carbon on the stress-strain behavior in the plain carbon steels for Zener-

Deiters .T. A, Mudawar .I, 1989, "Optimization of spray quenching for aluminum extrusion, forging, or continuous casting" Journal of Heat Treating, 7.1, pp. 9-18

Deiters .T.A and Mudawar .I, 1990, Prediction of the temperature-time cooling curves for three-dimensional aluminum products during spray quenching, J. Heat Treat. 8 81–91.

Den Ouden. C, Verhagen .C, and Tichelgar G.W. 1975. Influence of chemical composition on mild steel weld metal notch toughness. Welding journal'54 (3).87-s to 94-s.)

Drumond .J et.al (2012) Effect of Silicon Content on the Microstructure and Mechanical Properties of Dual-Phase Steels, Springer Science+Business Media New York and ASM International 2012

Estes .K.A and I. Mudawar, 1995 Correlation of Sauter mean diameter and critical heat flux for spray cooling of small surfaces, Int. J. Heat Mass Transfer 38 2985–2996.

Evans, CN. 1981. The effect of carbon on the microstructure and properties of C-Mn all- .weld metal deposits. IIW Doc. ll-A-546-81.)

Fadare. D.A, Fadara. T.G. and Akanbi.O.Y. 2011.Effect of Heat Treatment on Mechanical Properties and Microstructure of NST37-2 Steel.Journal of Minerals and Materials Characterization and Engineering, 10, 299-308.

Fernandes. P and Prabhu K.N, 2007 Effect of Section Size and Agitation on Heat Transfer during Quenching of AISI 1040 Steel. Journal of Materials Processing Technology,

Fish P. M. 1995 “utilization of low carbon steel” Wood head Pub. Ltd., Cambridge,

Flenner 2007, Carbon Steel Handbook. EPRI, Palo Alto, CA: 2007. 1014670

Grabke .H.J (1987), Effects of Impurities in Steels on Mechanical Properties and Corrosion Behavior, Steel Res., 1987, 58, p 477–482.

Haifeng XU et.al (2015) “Effects of Aluminium on the Microstructure and Mechanical Properties in 0.2C–5Mn Steels under Different Heat Treatment Conditions” ISIJ International, Vol. 55 (2015), No. 3, pp. 662–669

Hall .D.D, 1993, A Method of Predicting and Optimizing the Thermal History and Resulting Mechanical Properties of Aluminum Alloy Parts Subjected to Spray Quenching, MS Thesis, Mechanical Engineering, Purdue University, West Lafayette, IN,

Hall .D.D, and Mudawar .I, 1995, Predicting the impact of quenching on mechanical properties of complex-shaped aluminum alloy parts, J. Heat Transfer 117 479–488.

Hall .D.D. and Mudawar .I, 1996, optimization of Quench history of Aluminum Parts for Superior Mechanical Properties, Int. J. Heat Mass Transfer, Vol 39, p 81-95

Hall. D.D, Mudawar .I, Morgan .R.E, Ehlers .S.L, 1997, Validation of a systematic approach to modeling spray quenching of aluminum alloy extrusions, composites and continuous castings, J. Mater. Eng. Perform. 6 77–92.

Hassan .S.B, Agboola J.B, Aigbodion, V.S, and Williams. E.J 2010 Hardening Characteristics of Plain Carbon Steel and Ductile Cast Iron Using Neem Oil as Quenchant.Journal of Minerals and Materials Characterization andEngineering, 5, 31-36.

Honda .H, Takamastu .H, Wei .J.J, 2002, Enhanced boiling of FC-72 on silicon chips with micro-pin-fins and submicron-scale roughness, ASME J. Heat Transfer 124 383–389.

Huyett G.L 2004.Effect of Heat Treatment on Mechanical Properties and Microstructure of medium carbon Steel

Joseph BabalolaAgboola, OladiranAbubakreKamardeen, EdekiMudiare, Michael BolajiAdeyemi, 2015 “Effect of Velocity of Impact on Mechanical Properties and Microstructure of MediumCarbon Steel during Quenching Operations”

Kabir .I. R, Islam .M. A, 2014, Hardened Case Properties and Tensile Behaviours of TMT Steel Bars, American J. Mech. Eng. 2(1) 8-14.

Klinzing .W.P, Rozzi .J.C, Mudawar .I, 1992 Film and transition boiling correlations for quenching of hot surfaces with water sprays, J. Heat Treat. 9 91–103.

Kreyser .G and Eckermann .R (1992) DECHEMA Corrosion Handbook, Vol 11, Eds., VCH Publishers, New York, 1992, p 182
Lefebvre .A.H, 1989, “Atomization and Sprays cooling of metals” Hemisphere Publishing Corporation, New York

Leslie W.C,1987, The physical metallurgy of steels”, International student Ed., McGraw-Hill, Tokyo, Japan, pp. 135-182)

Leslie W.C. (1987),”The physical metallurgy of steels”, International student Ed., McGraw-Hill, Tokyo, Japan, 1987,pp. 135-182.

Manojkumar, Lakall .S, Dr.Chikalthankar .S.B,2012, “Improvement in Yield Strength of Deformed Steel Bar by Quenching Using Taguchi Method” ISSN: 2278-1684 Volume 2, Issue 2 (Sep.-Oct. PP 01-11 www.iosrjournals.org

Martini C, G. Palombarini, Poli G, and Prandstraller D, 2004. Wear 256, 608
Mead .H.W and Birchenal C. E, 1956. Trans. TMS AIME206, 1336

Merwin .M. J, 2007, Heat treatment of steel Mater. Sci. Forum, 539–543 4327. Sci. Eng.A, 532 435.

Mohammed. M. (2010) The Effect of Agitation and Quenchant Temperature on the Heat Transfer Coefficients for 6061 Aluminum Alloy Quenched in Distilled Water. Journal of ASTM International, 7, 189-194.

Mudawar .I and Valentine .W.S, 1989 Determination of the local quench curve for spray cooled metallic surfaces, J. Heat Treat. 7 107–121.

Mudawar.I and Estes K.A, 1996 Optimizing and predicting CHF in spray cooling of a square surface, J. Heat Transfer 118 672–680.

Murata .Y, Morinaga .M, Hashizuma. R, Takami. K, Azuma .T, Tanaka .Y, and Ishiguro T, 2000.Mater.Sci. Eng. A 282, 251

Musonda, 2017, Advances in Engineering Research (AER), volume 102 Second International Conference on Mechanics, Materials and Structural Engineering (ICMMSE)

Narayanasamy R, Anandakrishnan V, and Pandey K. S, 2008 Mater. Sci. Eng. A 494, 337

Park2004,Metals Handbook, Volume 9: Metallography and Microstructures,"Metallurgy and Microstructure," "Bainitic Structures." ASM International, Materials Park, OH.

Pickering F.B, 1978, Physical Metallurgy and the Design of Steels, 1978thedn.(Applied Science Publishers, London, p. 11 Hollomo (Z) conditions". Australia, p. 483.

Pola .A, Gelfi .M, La Vecchia .G. M, 2013, "Simulation and validation of spray quenching applied to heavy forgings", Journal of Materials Processing Technology, 213.12, pp. 2247-2253),

Rajan .T.V,Sharma .C.P, Ashok Sharma 1994, Heat Treatment Principles and Techniques.Revised edition. New Delhi: Prentice-Hall of India Private Limited.115

RamioSuorantaKote 2004, Material science handbook,

Raudensky .M, Chabicovsky .M, Hrabovsky. J, 2014, Impact of Oxide Scale on Heat Treatment of Steels, Proc. of the 23rd International Conference on Metallurgy and Materials, Brno, 553–558 3

Rybicki .J.R and Mudawar .I, 2006, Single-phase and two-phase cooling characteristics of upward-facing and downward-facing sprays, Int. J. Heat Mass Transfer 49 5–16.

Schöne .S, 2012 “ Integration des Düsenfeld-Gasabschreckens in den Strangpressprozess von Aluminiumlegierungen“, Dissertation Universität Rostock,

Schwabe .K and Arnold W.D. (1971), Behavior of Low Alloyed Steel, Proc. 5th Intl. Congress on Metallic Corrosion (Houston), NACE, 1971, p 760–763.

Shi.J, Sun .X. J, Wang .M. Q, Hui .W. J, Dong .H and Cao .W. Q 2010, “Effect of Heat Treatment on Mechanical Properties of Steel” Scr. Mater., 63 815.

Shizhong .W, Jinhua .Z and Long .R, 2006. Effect of Heat treatment Cycle on the Mechanical Properties Mater. Design,27, 1

Simon .P, Economopoulos. M and Nillies. P, 2017TEMPCORE, an economical process for the production of high-quality rebars”, reprint from MPT-Metallurgical Plant and Technology, 3(84) 80-93.

Smith W. F and Hashemi J, 2006 Foundations of Mater.Sci.and Eng., 4th ed., McGraw-Hill, Higher Education, Boston, p. 388

Song Zhen 2015, studied the “Effect of Heat Treatment on the Microstructure and Mechanical Properties of Steel”

Surian E. et al 1991 “influence of carbon on mechanical properties and microstructure of weld metal from a high-strength SMA electrode”,

Thome .J.R 1990, Enhanced Boiling Heat Transfer, Hemisphere Publishing Corporation, New York, NY,

Toda. S, 1972 A study in mist cooling (1st report: an investigation of mist cooling),Trans. JSME 38 581–588.

Totten .G.E, Bates .C.E, Clinton .N.A, 1993, .Handbook of Quenchants and Quenching Technology, ASM International, Materials Park, OH,

Ujereh S, Fisher T, Mudawar .I, 2007, Effects of carbon nanotube arrays on nucleate pool boiling, Int. J. Heat Mass Transfer 50 4023–4038.)

Valeria et al 2015 in the study of effects of carbon content on microstructure and mechanical properties of dual phase steels

Wang .C, Shi J, Wang .C. Y, Hui. W. J, Wang .M. Q, Don .H and Cao .W. Q 2011, ISIJ Int., 51 651. an overview on high manganese steel casting", proceeding of the world foundry congress. Spain Bilbao

Willey W.L and L.A, 1948, Quenching of 75S Aluminum Alloy Trans. AIME, Vol 175, p414-427

Xu. H. F, Zhao.J, Cao. W. Q, Shi .J, Wang .C. Y, Wang. C, Li .J and Dong .H 2012, Mater C. Y. Wang, J. Shi, W. Q. Cao and H. Dong: (2010), Mater. Sci. Eng.A, 527 3442.

Xuan.Y, Li .Q, 2000, Heat transfer enhancement of nanofluids, Int. J. Heat Fluid Flow 21 58–64).

Yamashita .M, et.al (1998), Structure of Protective Rust Layers Formed on Weathering Steels by Long Term Exposures in the Industrial Atmosphere of Japan and North America, Iron Steel Inst. Jpn. Int., 1998, 38, p 285–290

Yi .H. L, Lee. K. Y and Bhadeshia .H. K. D. H 2011, Effects of Aluminium on the Microstructure and Mechanical Properties in low carbon Steels under Different Heat Treatment Conditions" Mater. Sci. Eng.A, 528 5900.

Yoo .O, Ohb .Y. J, Lee .B. S and Nama .S.W, 2005.Mater.Sci. Eng. A 405, 147

APPENDICES

Appendix 1: Activity Plan/ Schedule

Activity / Month	Period 2018											
	1	2	3	4	5	6	7	8	9	10	11	12
	Jan	Feb	Mar	Apr	May	June	Jul	Aug	Sept	Oct	Nov	Dec
Thesis report writing												
Research Thesis report submission												
Thesis report presentation and Approval												
1st publication submission												
Data collection & Analysis												
Master Thesis writing												
Master Thesis submission												
Master Thesis defense												

Appendix 2: Experimental design of cooling batch B (12 mm rebar)

Pre-set Cooling condition (parameters)		
S.N	Coolant temperature [^{0}C]	Coolant pressure [Kgf/cm^2]
1	25	10
2	25	10
3	25	10
4	35	10
5	35	10
6	35	10
7	45	10
8	45	10
9	45	10
10	35	5
11	35	5
12	35	5
13	35	14
14	35	14
15	35	14

Appendix 3: Experimental design of cooling batch D (16 mm rebar)

Pre-set cooling condition (parameters)		
S.N	Coolant temperature [^{0}C]	Coolant pressure [Kgf/cm^2]
1	25	10
2	25	10
3	25	10
4	35	10
5	35	10
6	35	10
7	45	10
8	45	10
9	45	10
10	35	5
11	35	5
12	35	5
13	35	14
14	35	14
15	35	14

Appendix 4: Experimental design of cooling batch C (20 mm rebar)

Pre-set cooling condition (parameters)		
S.N	Coolant temperature [^{0}C]	Coolant pressure [Kgf/cm^2]
1	25	10
2	25	10
3	25	10
4	35	10
5	35	10
6	35	10
7	45	10
8	45	10
9	45	10
10	35	5
11	35	5
12	35	5
13	35	14
14	35	14
15	35	14

Appendix 5:Experimental design and tensile test results.

S.N	Rebar size [mm]	Coolant temp [^{0}C]	Coolant pressure [Kgf/cm^2]	UTS [MPa]	YS [MPa]	Elongation [%]
1	12	25	10	686	581.36	12.01
2	12	25	10	685	580.51	12
3	12	25	10	687	582.2	12.02
4	12	35	10	648.5	544.96	23.05
5	12	35	10	648	544.54	23
6	12	35	10	647.5	544.12	22.99
7	12	45	10	546	527.22	45
8	12	45	10	542	528.14	47
9	12	45	10	537	518.44	49
10	12	35	5	533	480.18	50
11	12	35	5	538	484.68	48.2
12	12	35	5	544	490.09	46
13	12	35	14	542	483.93	47.05
14	12	35	14	540	482.14	46.2
15	12	35	14	537	479.46	48.05
1	16	25	10	663.5	548.35	16.6
2	16	25	10	664	548.76	16.1
3	16	25	10	665.5	550	15.6
4	16	35	10	604	516.24	31.6
5	16	35	10	604	516.24	31.6
6	16	35	10	604	516.24	31.6
7	16	45	10	547.8	445.37	47.6
8	16	45	10	547	444.72	47.8
9	16	45	10	546.2	444.07	48.01
10	16	35	5	530.4	442	49.3
11	16	35	5	530	441.67	49.8

12	16	35	5	529.6	441.33	50.3
13	16	35	14	534	476.79	49.1
14	16	35	14	535	477.68	48.9
15	16	35	14	536	478.57	48.7
1	20	25	10	652.35	572.24	18.01
2	20	25	10	652	571.93	18.3
3	20	25	10	651.65	571.62	18.59
4	20	35	10	557	484.35	34
5	20	35	10	557	484.35	34
6	20	35	10	557	484.35	34
7	20	45	10	549.93	423.02	45.44
8	20	45	10	549	422.3	45.8
9	20	45	10	548.07	421.59	46.16
10	20	35	5	522	383.8	55.6
11	20	35	5	522	383.8	55.6
12	20	35	5	522	383.8	55.6
13	20	35	14	528.6	412.97	53.1
14	20	35	14	528	412.5	53.4
15	20	35	14	527.4	412.03	53.7

Appendix 6: Adjusted experimental design and tensile test results.

S.N	Rebar size [mm]	Coolant temperature [^{0}C]	Coolant pressure [Kgf/cm^2]	UTS [MPa]	YS [MPa]	UTS:YS	Elongation [%]
1	12	33.5	10	648.04	544.54	1.19	23
2	12	44.5	14	556.035	479.31	1.16	42
3	16	35.5	6.8	553.85	481.74	1.15	43.4
4	16	44.5	13.2	643.09	549.57	1.17	25.1
5	20	26	6.3	557.79	481.03	1.16	41.5
6	20	43	13.3	645.063	546.61	1.18	24.8

Appendix 7 : Tensile test certificates for the specimen.

Test Certificate

Name of Company : ROOFINGS ROLLING MILLS LTD.
Address : P.O.BOX 35086, KAMPALA, UGANDA
To :
Sample Identification : RRM 16MM,TMT
Machine : FIE Make Universal Testing Machine, UTE-100

Input Data : File Name : 27-9-2018-16MM-MSC-3D , Record No. : 1 , Date : 27-09-2018
: Sample Type -- TMT , Area : 198.266 mm ²
: Length = 532.0 mm , Weight = 0.828 kg
: Gauge Length : 80 mm Final Gauge Length: 130 mm

Results of : Tension Test

Maximum Force (Fm)	: 79.000 kN	Yield Stress	: 0.257 kN/mm ²
Disp. at Fm	: 65.400 mm	UTS/YS Ratio	: 1.552
Max. Disp.	: 81.900 mm		
Tensile Strength (Rm)	: 0.398 kN/mm ²		
Elongation	: 62.500 %		
Yield Load	: 50.900 kN		

* Note : Yield Calculated from graph

Graph : Load Vs Displacement

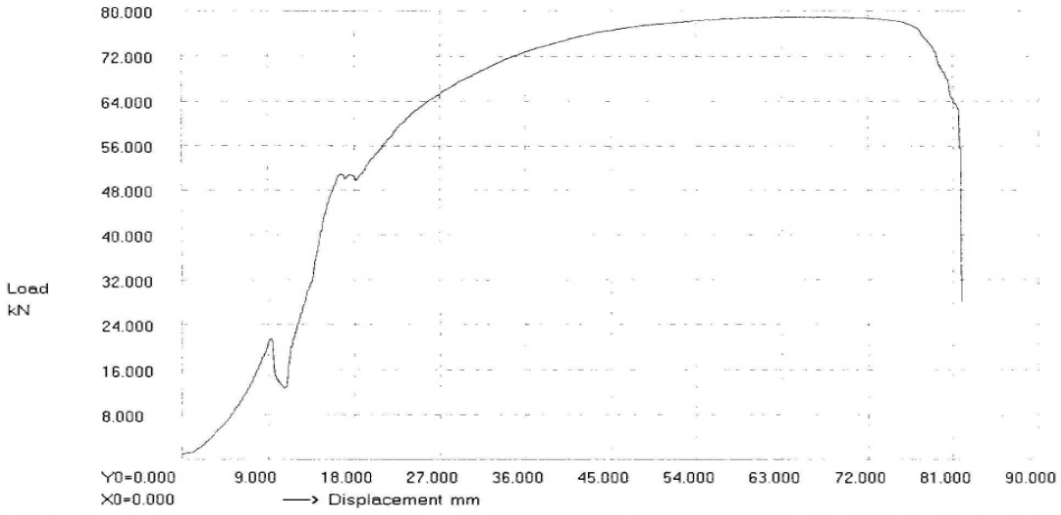

For ROOFINGS ROLLING MILLS LTD.

Test Certificate

Name of Company : ROOFINGS ROLLING MILLS LTD.
Address : P.O.BOX 35086, KAMPALA, UGANDA
To :
Sample Identification : RRM 16MM TMT
Machine : FIE Make Universal Testing Machine, UTE-100

Input Data : File Name : 26-09-2018-16MM-MSC-1D , Record No. : 1 , Date : 26-09-2018
: Sample Type -- TMT , Area : 198.108 mm ²
: Length = 544.0 mm , Weight = 0.846 kg
: Gauge Length : 80 mm Final Gauge Length: 114 mm

Results of : Tension Test

Maximum Force (Fm)	: 126.000 kN	Yield Stress	: 0.533 kN/mm ²
Disp. at Fm	: 42.900 mm	UTS/YS Ratio	: 1.194
Max. Disp.	: 50.100 mm		
Tensile Strength (Rm)	: 0.636 kN/mm ²		
Elongation	: 42.500 %		
Yield Load	: 105.550 kN		

* Note : Yield Calculated By Offset method as per ASTM E8 at .5 % Strain offset

Graph : Load Vs Displacement

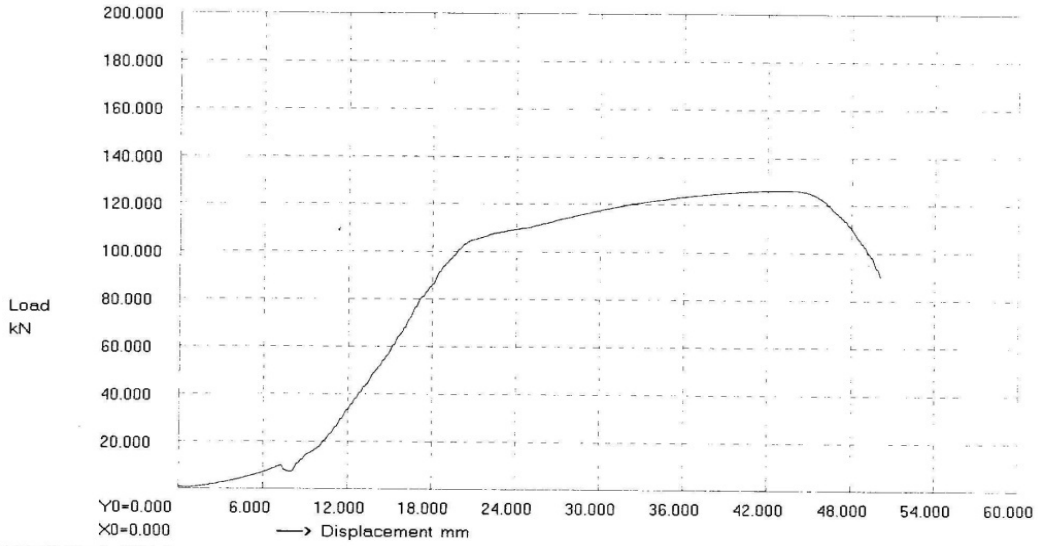

For ROOFINGS ROLLING MILLS LTD.

Test Certificate

Name of Company : ROOFINGS ROLLING MILLS LTD.
Address : P.O.BOX 35086, KAMPALA, UGANDA
To :
Sample Identification : RRM 20MM TMT
Machine : FIE Make Universal Testing Machine, UTE-100

Input Data : File Name : 26-09-2018-20MM-MSC-5C , Record No. : 1 , Date : 26-09-2018
: Sample Type -- TMT , Area : 309.240 mm ²
: Length = 414.0 mm , Weight = 1.005 kg
: Gauge Length : 100 mm Final Gauge Length: 118 mm

Results of : Tension Test

Maximum Force (Fm)	: 190.400 kN	Yield Stress	: 0.506 kN/mm ²
Disp. at Fm	: 44.800 mm	UTS/YS Ratio	: 1.217
Max. Disp.	: 53.200 mm		
Tensile Strength (Rm)	: 0.616 kN/mm ²		
Elongation	: 18.000 %		
Yield Load	: 156.450 kN		

* Note : Yield Calculated By Offset method as per ASTM E8 at 2 % Strain offset

Graph : Load Vs Displacement

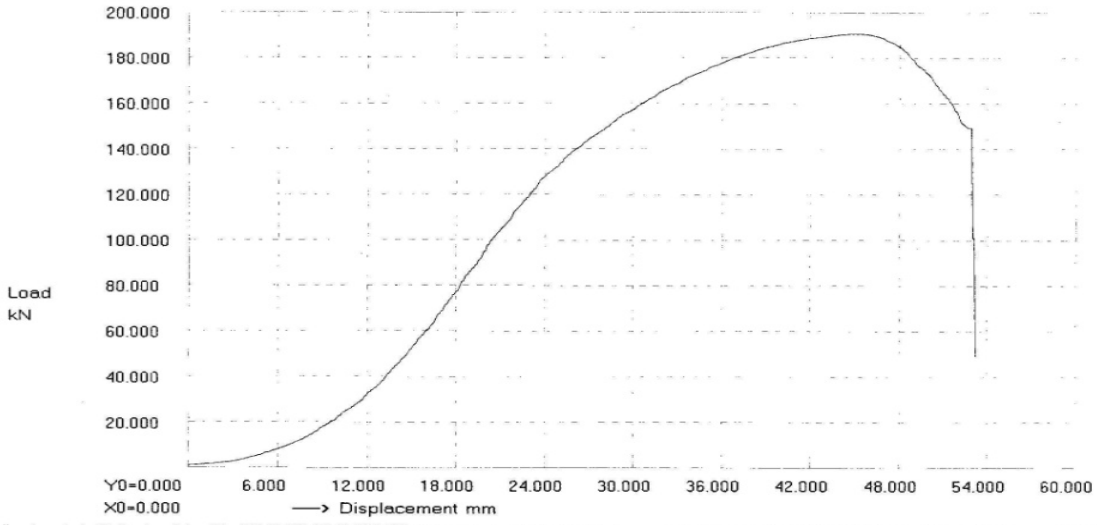

For ROOFINGS ROLLING MILLS LTD.

Test Certificate

Name of Company : ROOFINGS ROLLING MILLS LTD.
Address : P.O.BOX 35086, KAMPALA, UGANDA

To :

Sample Identification : RRM 20MM.TMT

Machine : FIE Make Universal Testing Machine, UTE-100

Input Data : File Name : 26-09-2018-MSC-1C . Record No. : 1 . Date : 26-09-2018
: Sample Type -- TMT . Area : 316.646 mm ²
: Length = 628.0 mm . Weight = 1.561 kg
: Gauge Length : 100 mm Final Gauge Length: 118 mm

Results of : Tension Test

Maximum Force (Fm)	: 209.550 kN	Yield Stress	: 0.569 kN/mm ²
Disp. at Fm	: 60.100 mm	UTS/YS Ratio	: 1.164
Max. Disp.	: 73.200 mm		
Tensile Strength (Rm)	: 0.662 kN/mm ²		
Elongation	: 18.000 %		
Yield Load	: 180.050 kN		

* Note : Yield Calculated By Offset method as per ASTM E8 at .8 % Strain offset

Graph : Load Vs Displacement

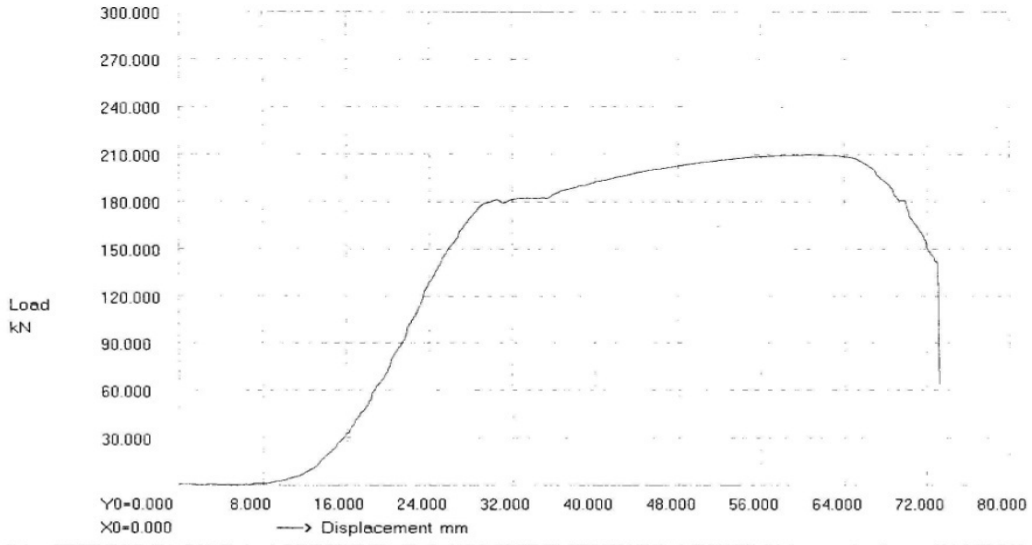

For ROOFINGS ROLLING MILLS LTD.

Appendix 8: Chemical analysis report

ROOFINGS ROLLING MILLS

1 September 2018

Method: Fe-10-F
Comment: Low alloy Steel
Element concentration
1 September 2018
Heat Number:
Sample ID: B
Analyst Name: OMARA
Quality Control Sample:

	C	Si	Mn	P	S	Cr	Mo	Ni
	%	%	%	%	%	%	%	%
Ø (2)	0.233	0.313	0.746	0.0350	0.0496	0.0764	0.0099	0.0411

	Al	Co	Cu	Nb	Ti	V	W	Pb
	%	%	%	%	%	%	%	%
Ø (2)	0.0229	0.0018	0.0917	< 0.0010	0.0014	0.0018	< 0.0100	0.0038

	Sn	As	Zr	Bi	Ca	Ce	B	Zn
	%	%	%	%	%	%	%	%
Ø (2)	0.0151	0.0147	< 0.0015	< 0.0040	> 0.0156	< 0.0030	0.0048	0.0195

	La	Fe	Sb	Te
	%	%	%	%
Ø (2)	0.0030	98.3	< 0.0010	< 0.0010

- 1 -